

Multiscale modeling of field-effect nano-sensors

Clemens Heitzinger

Department of Mathematics & Wolfgang Pauli Institute,
University of Vienna

Workshop *Kinetic description of multiscale phenomena*
March 4, 2009



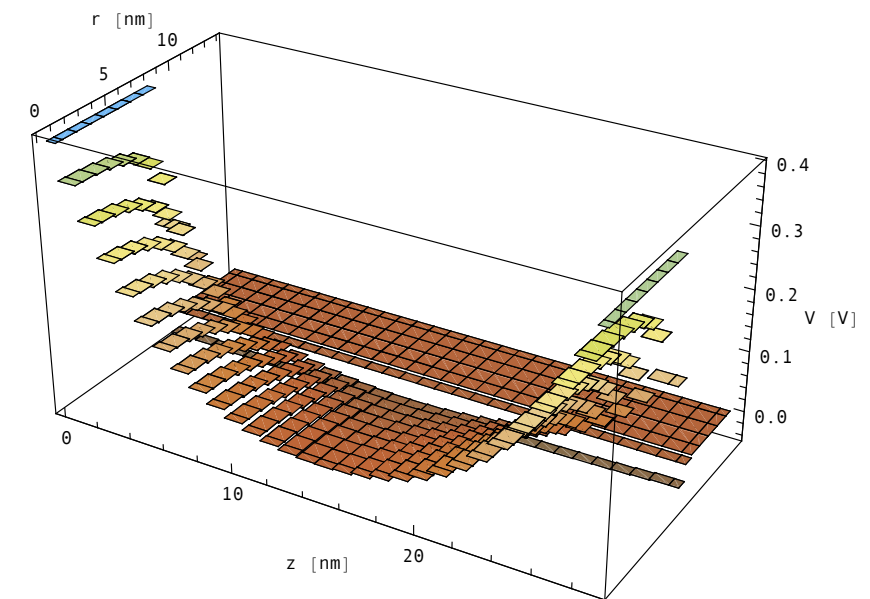
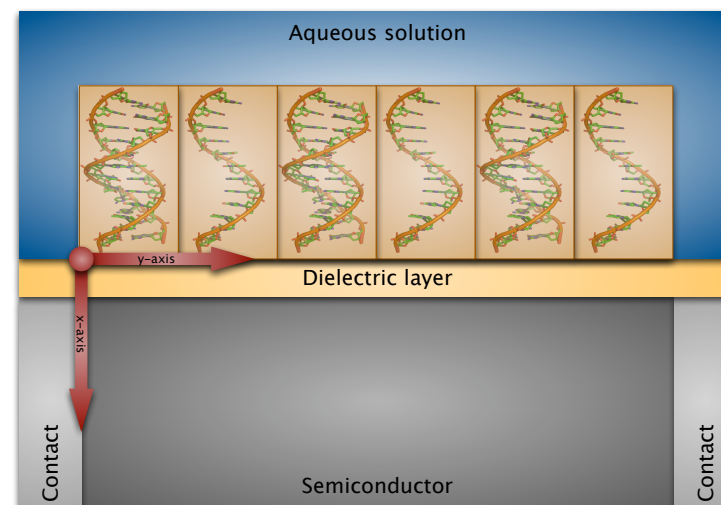
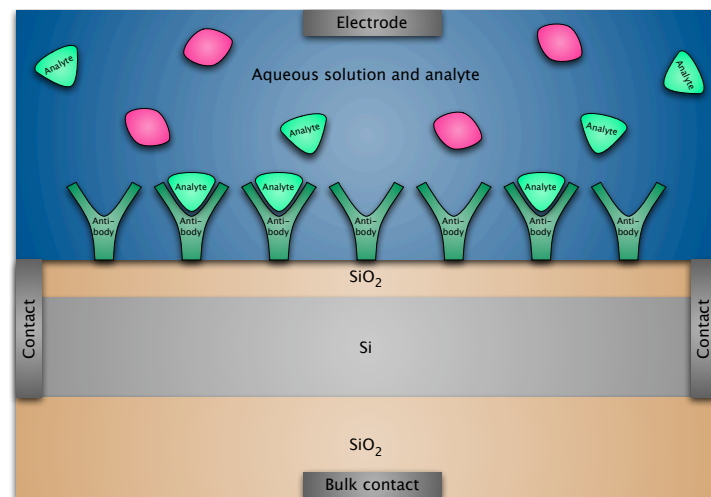
universität
wien

Overview

(1) Introduction to field-effect biosensors (or BioFETs)

(2) Methods & models: multi-scale modeling & self-consistent simulations

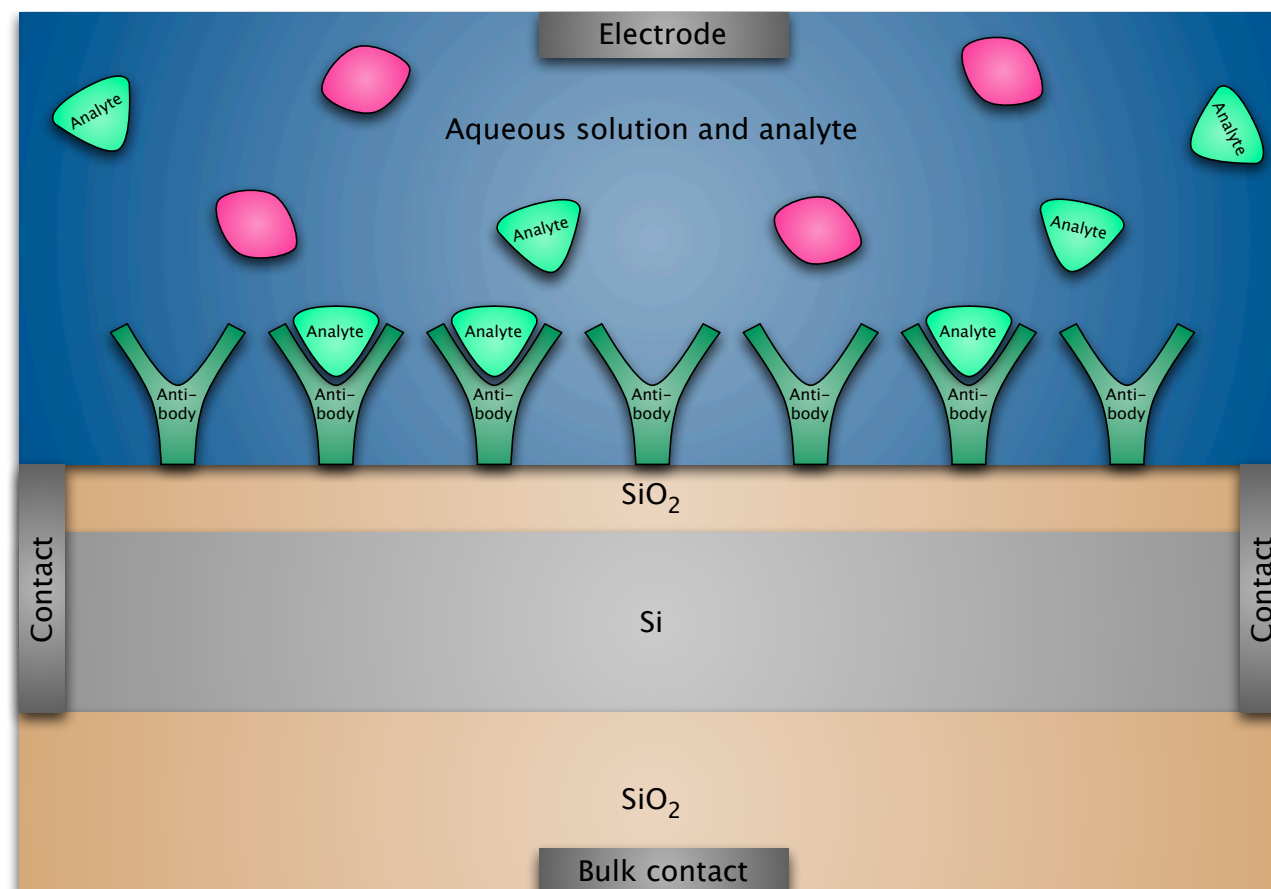
(3) Further developments, results & discussion



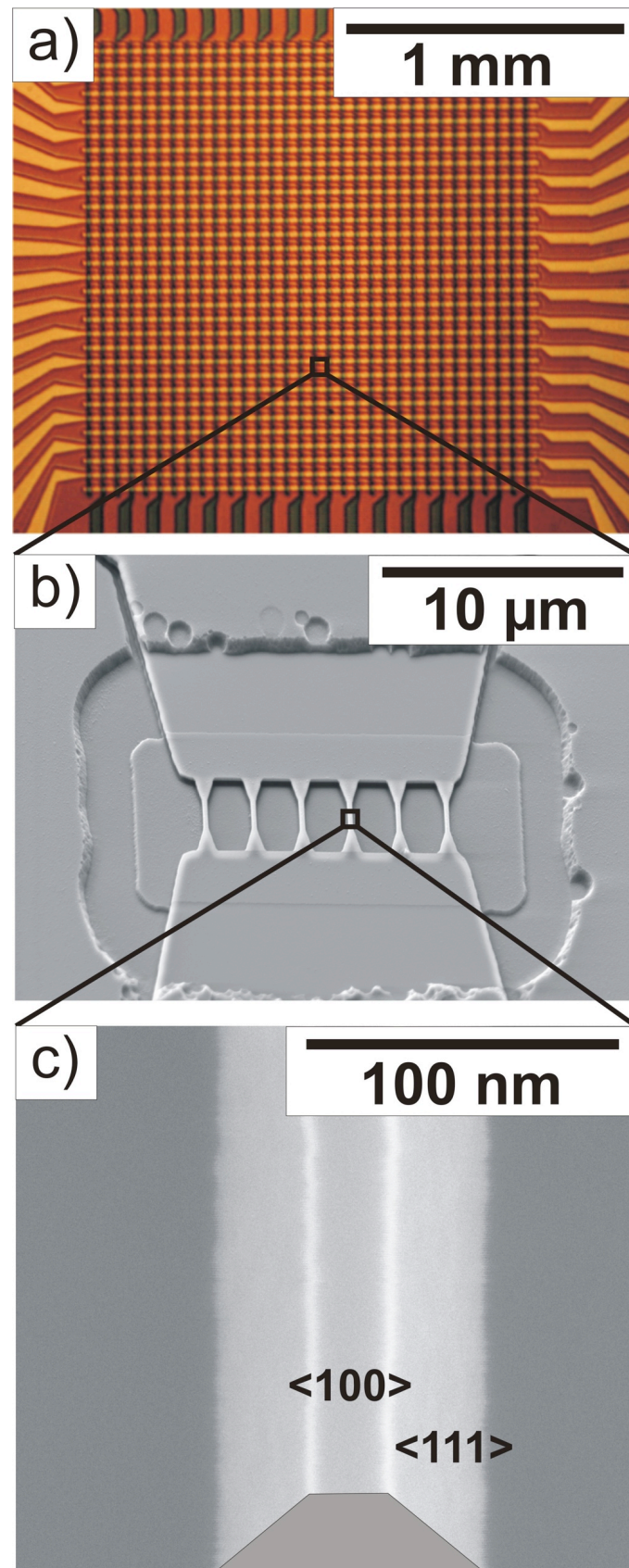
BioFETs are field-effect biosensors with semiconductor transducers

Biologically sensitive field-effect transistors (BioFETs) consists of three parts:

- **Receptor:** molecular recognition by functionalized surface.
- **Transducer:** performs the measurement. For example Si nanoplates or Si nanowires.
- **Signal processing.**



What a biosensor chip looks like



Length scale 1mm:

(a) shows the array of 32 x 32 sensors on the chip.

Length scale 10μm:

(b) shows a single sensor element. It consists of 6 nanowires.

Length scale 100nm:

(c) shows a single silicon nanowire with a trapezoidal cross section.

Sven Ingebrandt (Fachhochschule Kaiserslautern),
Andreas Offenhäusser (Forschungszentrum Jülich)



universität
wien

What are the advantages of BioFETs compared to current technology?

Current technology uses fluorescent or radioactive markers.

The main advantage of field-effect devices is direct, **label-free operation** (no markers are necessary).

Additional advantages are:

- Real-time & continuous sensing.
- No markers change the behavior of the analyte.
- The analyte can be re-used in subsequent experimental steps.
- Read-out circuitry & amplification can be integrated on the chip, which will be important for point-of-care applications.



The BioFET concept is a general one with many applications

There are numerous applications depending on how the surface was functionalized:

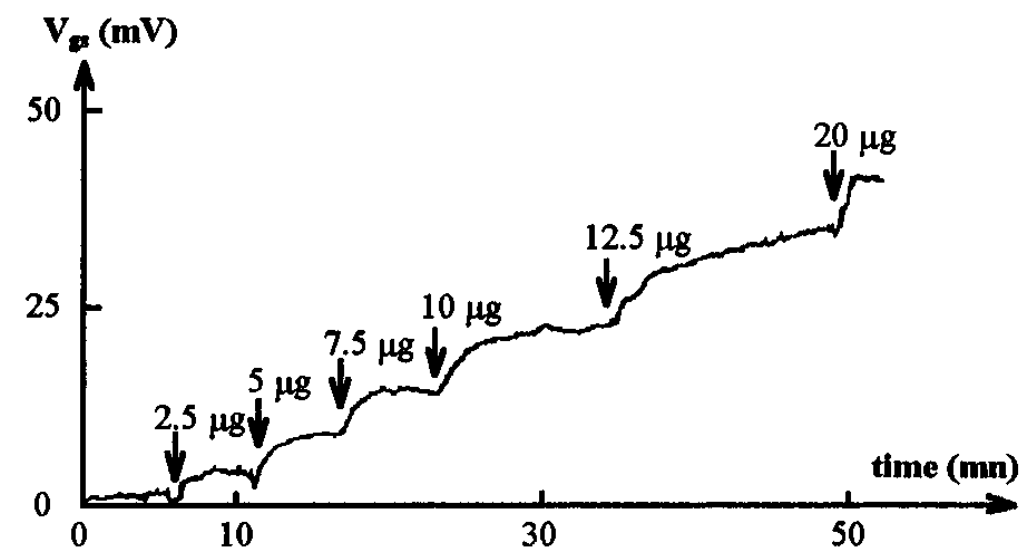
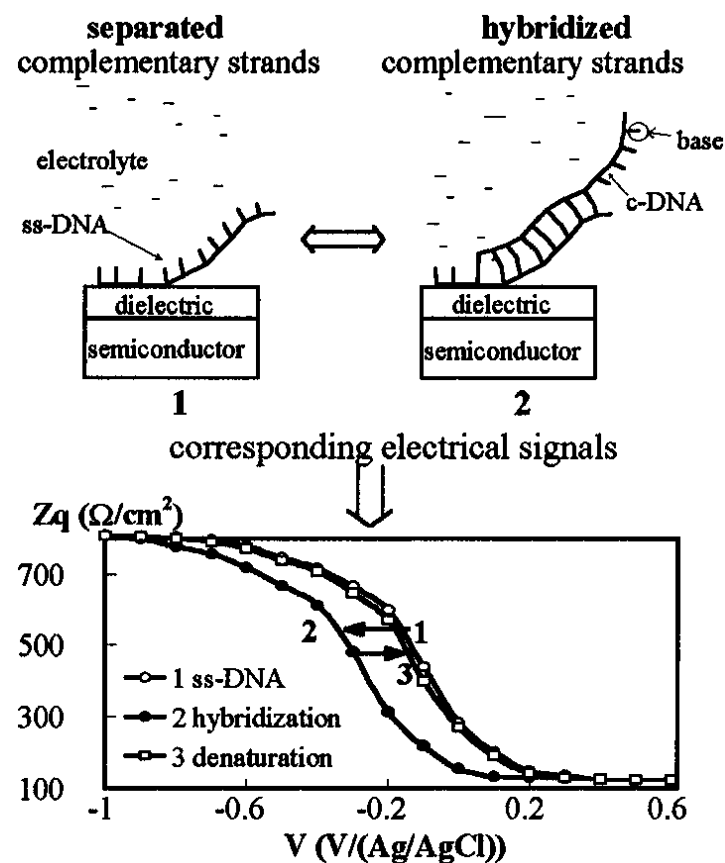
- Screening for dozens of tumor markers simultaneously (relative change is important).
- Detection of SNPs:
inherited diseases (like cystic fibrosis, which is one of the most common ones), cancer risk, etc.
- Detection of epigenetic modifications.
- Point-of-care applications
(NIH's 3 Ps: predictive, personalized, & preemptive medicine).
- DNA sequencing.



A DNA-FET was reported about 10 years ago

The first functional DNA-FET was manufactured in 1997:

- Sensor area: $20\mu\text{m} \times 500\mu\text{m}$, conventional device structure.
- Aqueous solution: pH 7.1 (buffered), 50mM NaCl.
- DNA strands used:
oligonucleotides: 18 base pairs,
polynucleotides: ca. 1000 base pairs.



Time dependence

(From: Souteyrand et al., J. Phys. Chem. B, **101** 1997)

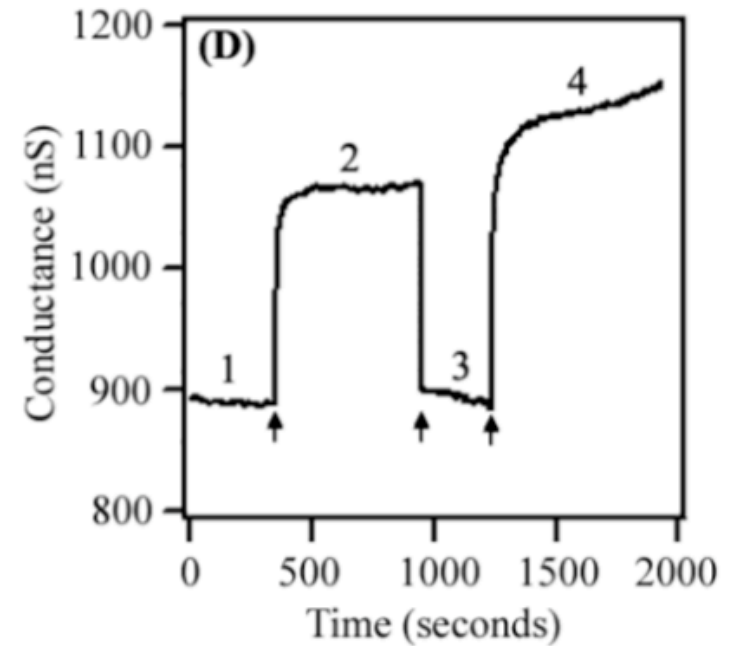
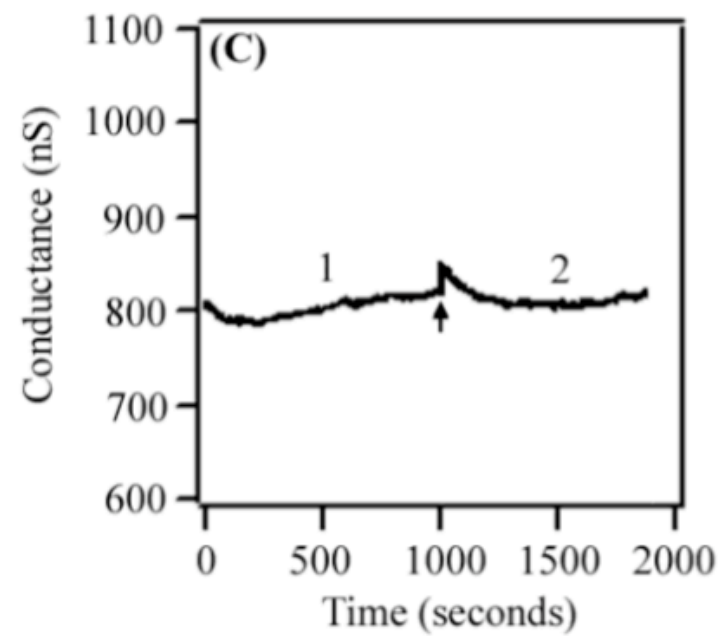
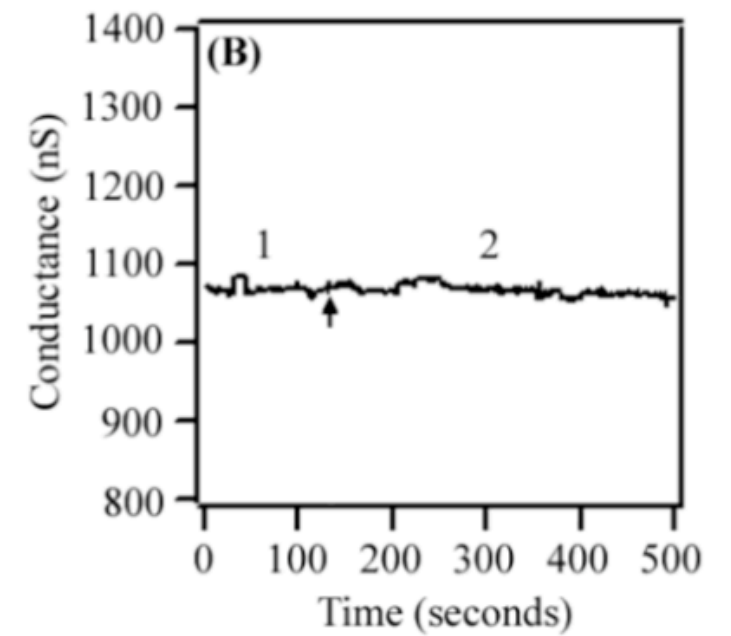
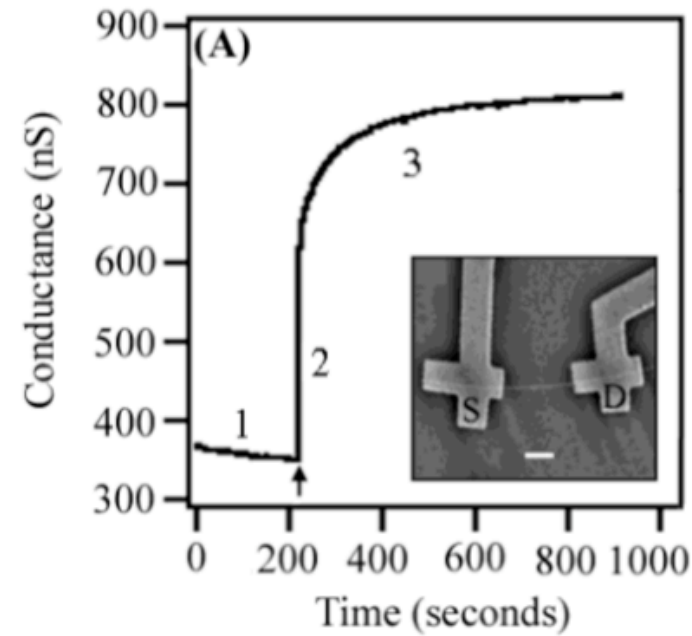
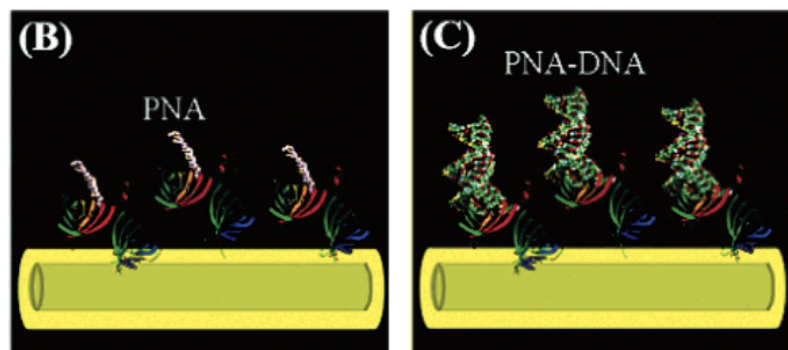
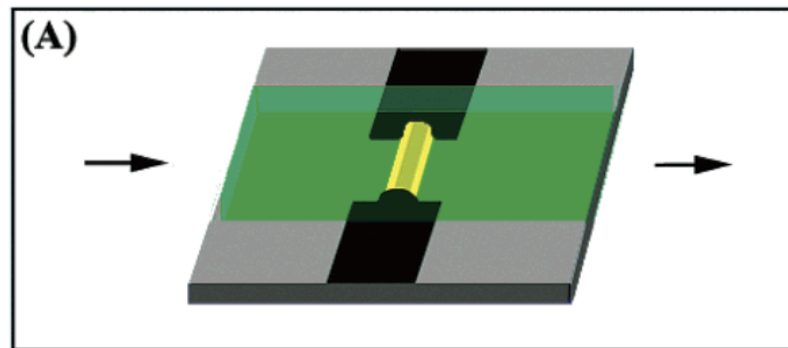


universität
wien

Silicon nanowire DNA-sensor

Silicon nanowires were grown in the vapor-liquid-solid growth mode.

Note the conductance change in (D) of about 15% to 20%.



(From: Hahm, Lieber, Nano Lett. 4 2004)

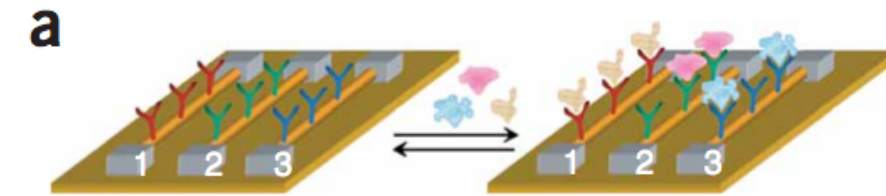


universität
wien

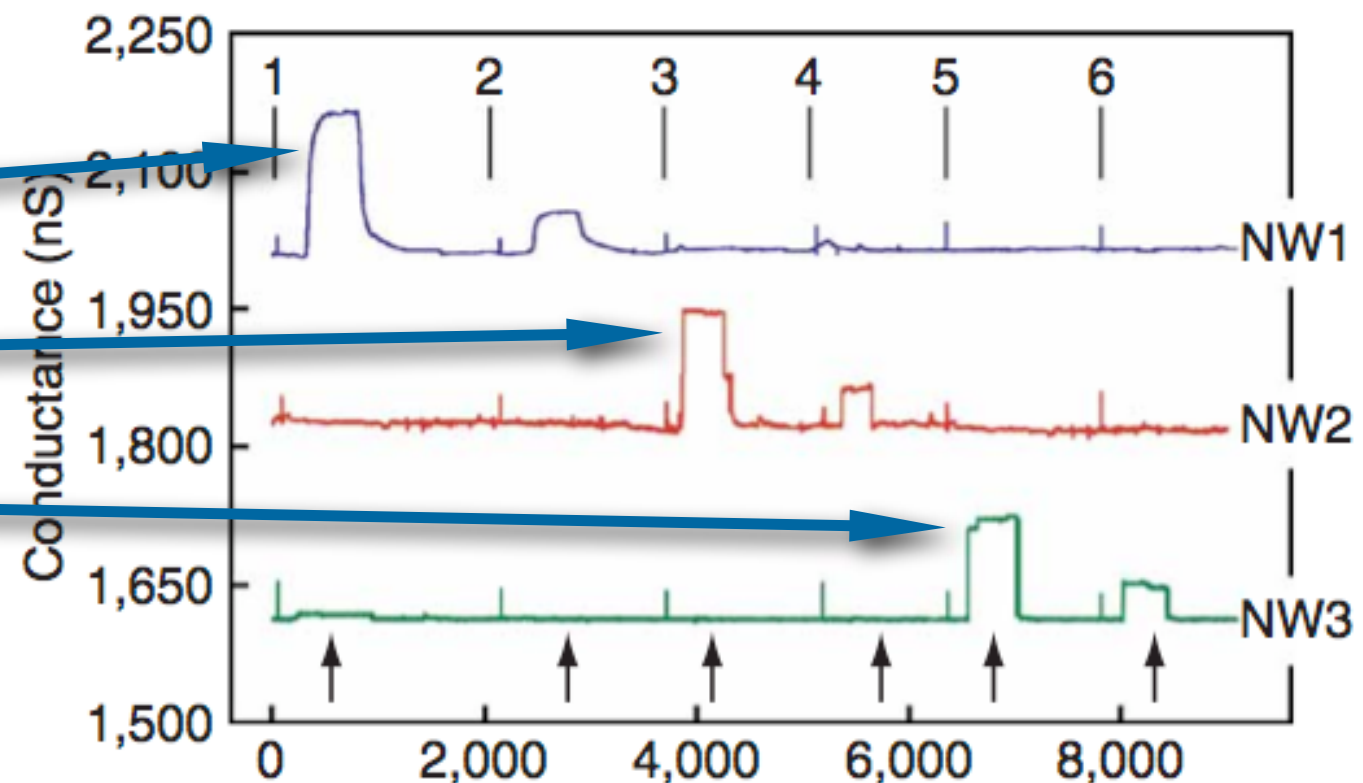
Tumor marker detection using Si nanowires

Arrays of silicon-nanowire ImmunoFETs enable highly sensitive (0.9pg/ml) detection of cancer markers:

- PSA (prostate specific antigen): increased levels indicate localized or metastatic prostate cancer.
- CEA (carcinoembryonic antigen): a glycoprotein involved in cell adhesion; increased levels indicate colorectal cancer.
- Mucin-1.



- (1) 0.9ng/ml PSA
- (2) 1.4pg/ml PSA
- (3) 0.2ng/ml CEA
- (4) 2.0pg/ml CEA
- (5) 0.5ng/ml mucin-1
- (6) 5.0pg/ml mucin-1



(From: Zheng et al., nature biotechnology **23** 2005)



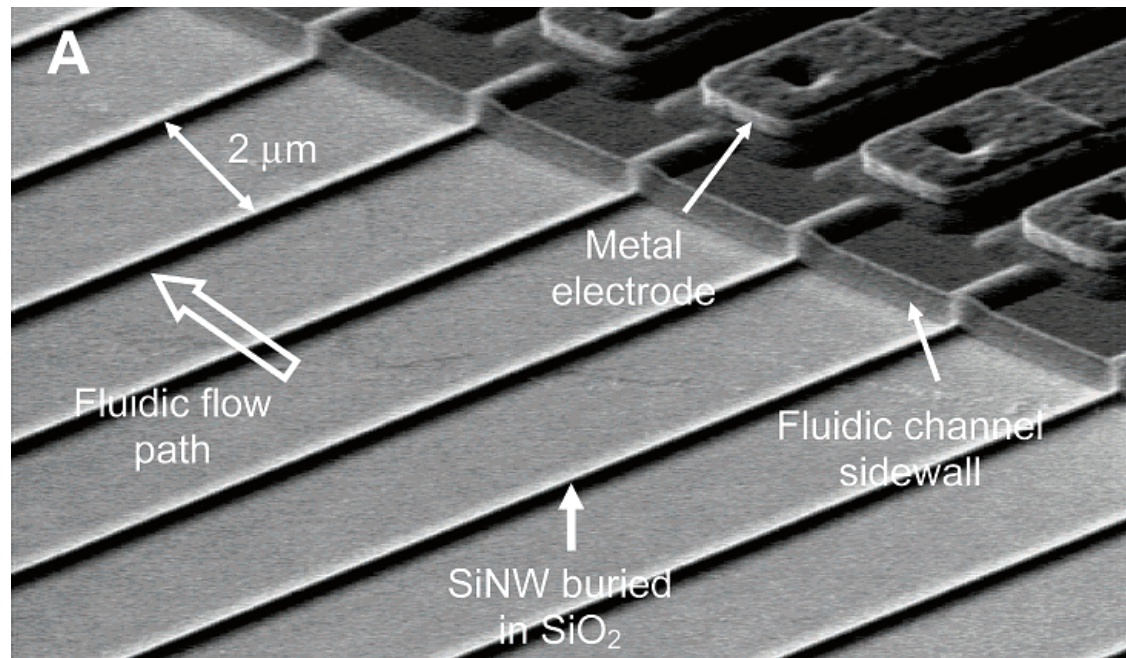
DNA detection using Si nanowires in arrays

PNA (peptide nucleic acid) probes were used to detect ssDNA.

The sensors discriminate satisfactorily against mismatched target DNA.

Detection limit of 10 fM.

Response time is not very good.



(From: Gao et al., Analytical Chemistry 79 2007)

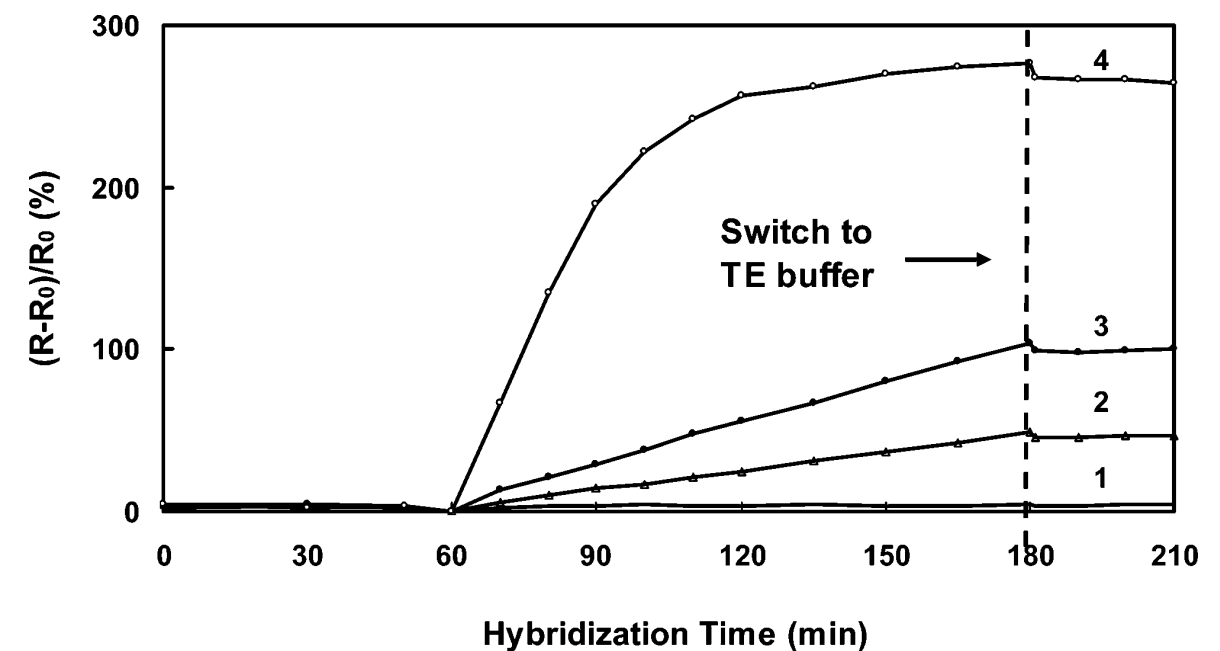


Figure 5. The dependence of resistance change of the SiNW array biosensor on hybridization time in (1) 1.0 nM control, (2) 25 fM, (3) 100 fM and (4) 1.0 nM target DNA in TE buffer.



Antigen detection using Si nanowires

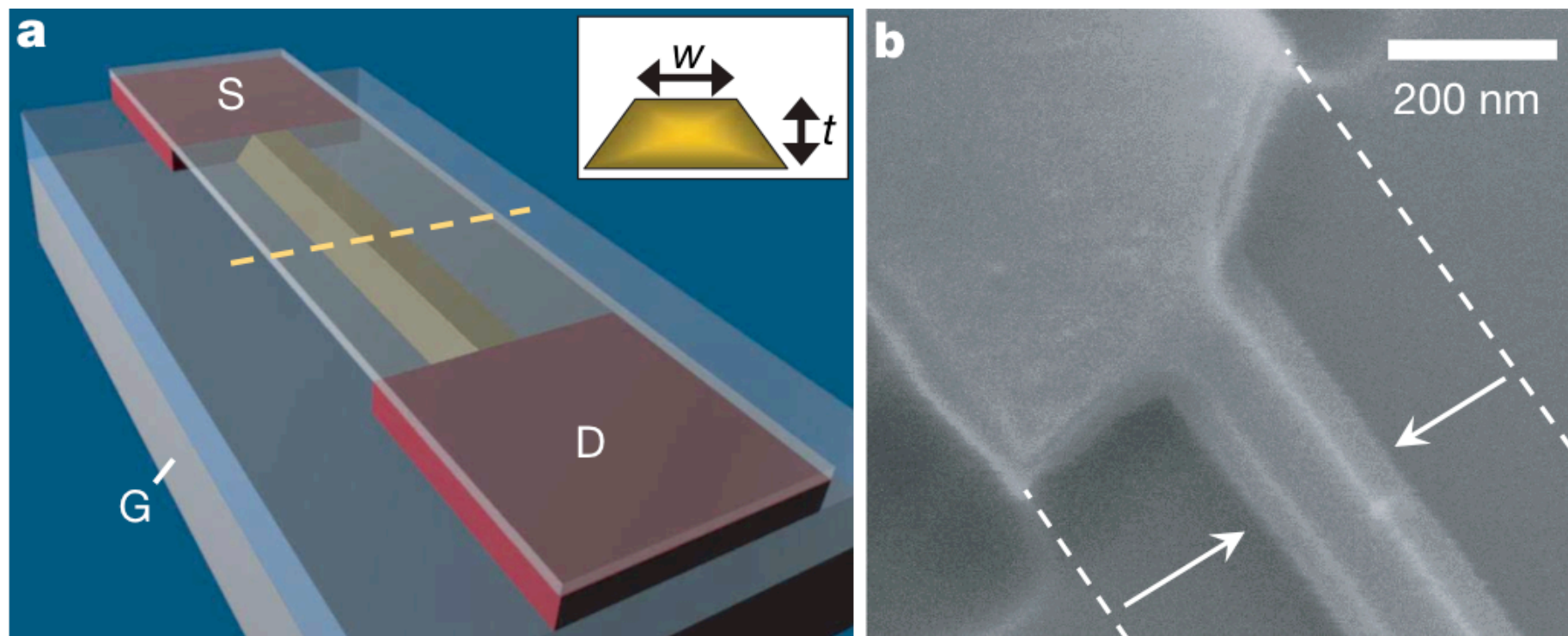
Traditionally, nanowires are made in the vapor-liquid-solid growth mode and assembled.

However, assembly is very time-consuming.

Here Si nanowires were fabricated in a top-down **CMOS-compatible** approach.

- Si nanowires: 40nm thick and 50nm to 150nm wide.
- Surface receptors: antibodies.
- 10fM concentrations of treptavidin were detected.

Special microfluidic channel and pump for fast response time.



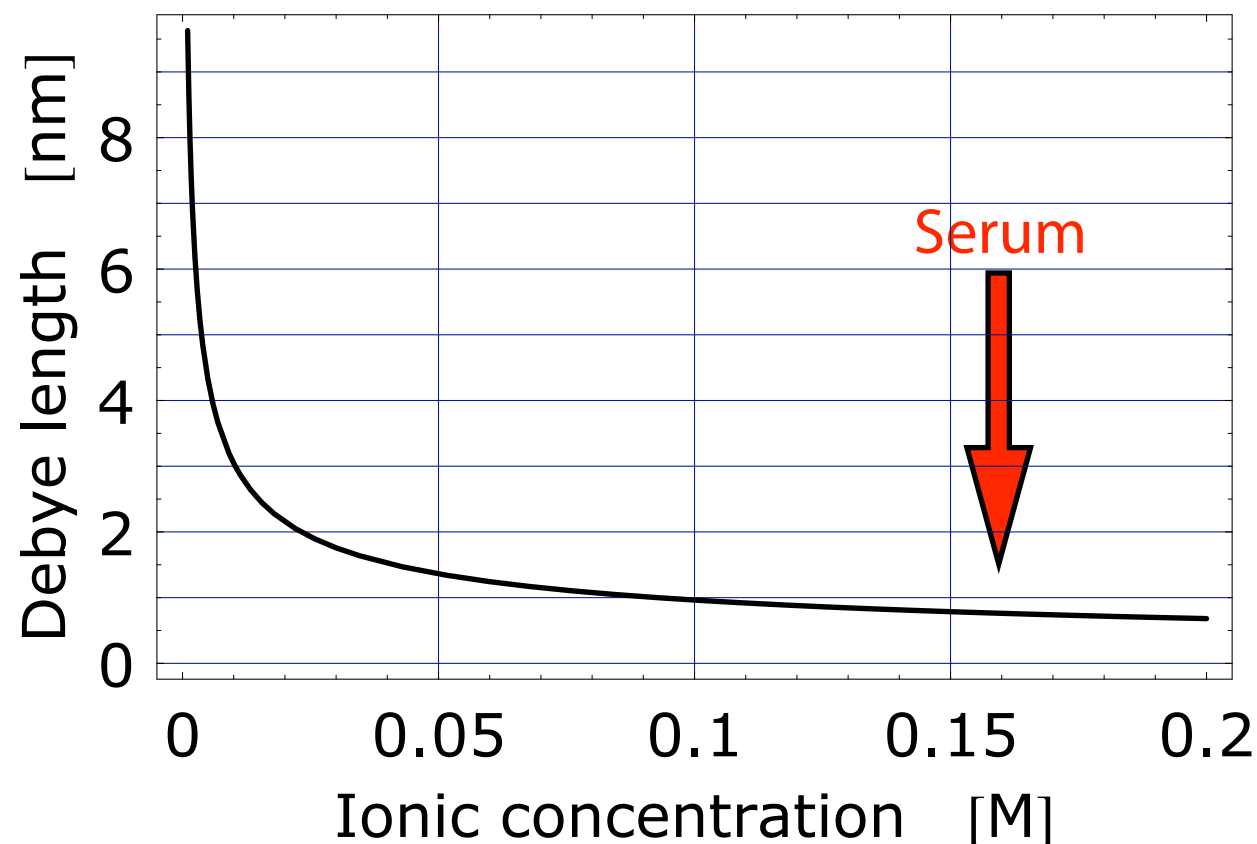
(From: Stern et al.,
nature **445** 2007)

An important question: the Debye length

The Debye length is the mean distance where the effect of a charge can be noticed.

It is ca. 1 nm at physiologically relevant concentrations (serum: ca. 160mM).

Therefore it was believed for a long time that field-effect sensors would not work.



The model hierarchy and modeling issues

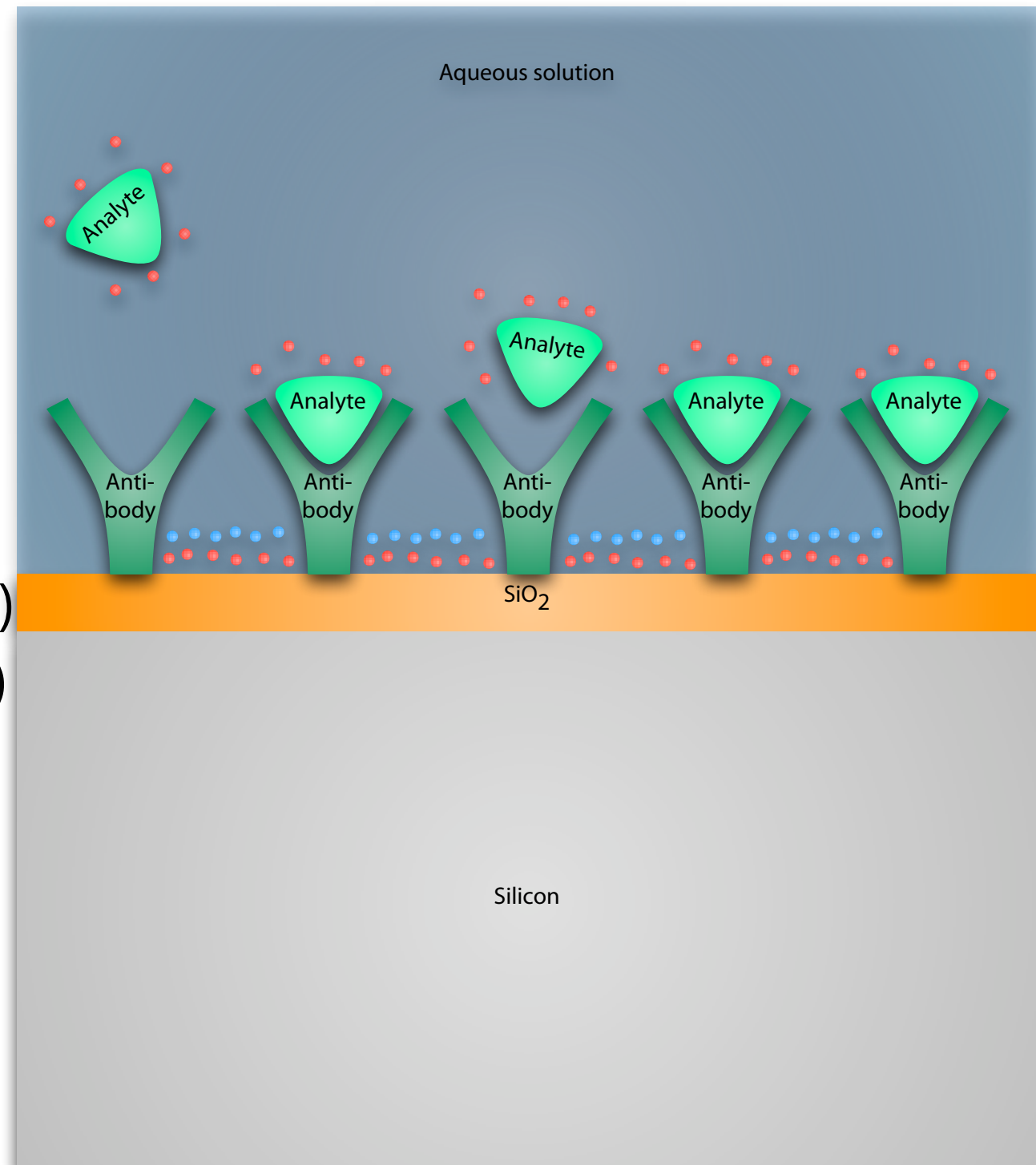
Electrostatics are governed by the **Poisson equation**:

$$-\partial_x (\epsilon(x) \partial_x V(x, \mathbf{y})) - \nabla_{\mathbf{y}} \cdot (\epsilon(x) \nabla_{\mathbf{y}} V(x, \mathbf{y})) = n_T(V(x, \mathbf{y}), x, \mathbf{y}) + n_E(x, \mathbf{y})$$

Self-consistent modeling of:

- **Biophysical part:**
 - Continuum model:
Poisson–Boltzmann equation
 - Atomistic model:
(Metropolis) Monte Carlo simulations
- **Nano-electronic part:**
 - Classical models:
 - drift-diffusion (with QM corrections)
 - Boltzmann equation (with QM corr.)
 - Quantum-mechanical models:
 - Effective quantum potentials
 - Non-equilibrium Green functions
 - Wigner functions

Our **multi-scale model** enables us to link the microscopic and macroscopic picture.



The multi-scale problem

We are dealing with two different length scales:

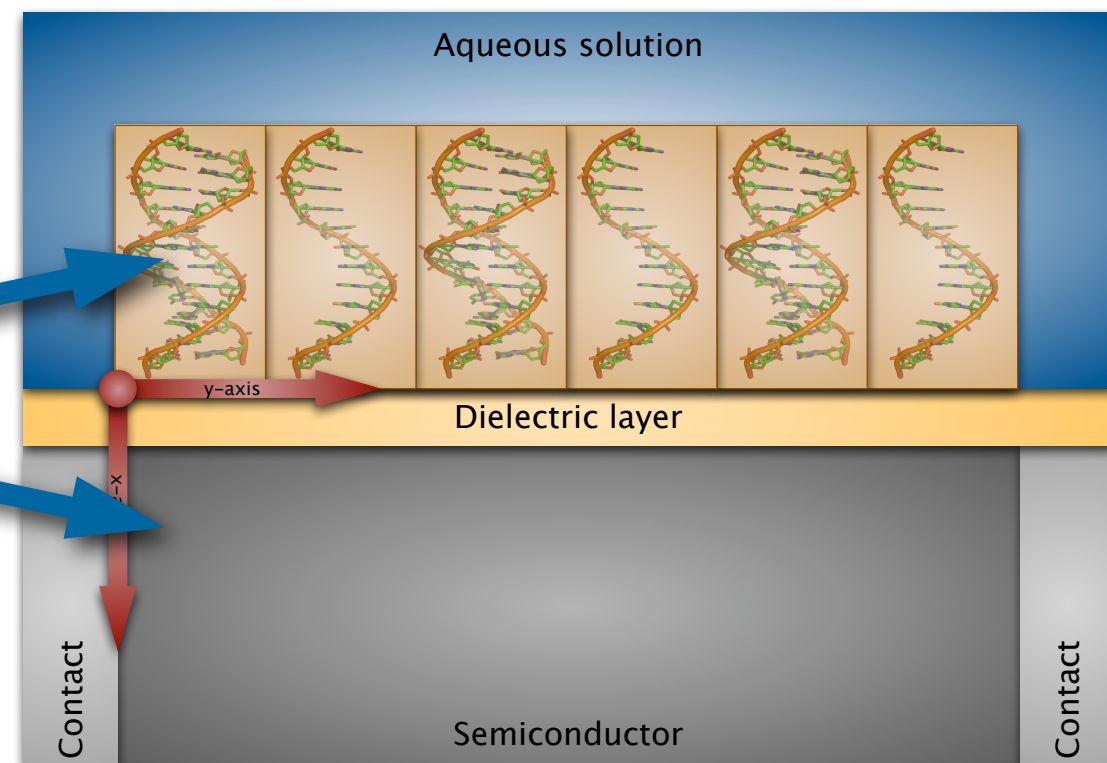
- DNA diameter: 2nm; hence the electrostatic potential around the biomolecules varies on the Angstrom scale;
- length of the sensor area: a few micrometer.

Simple idea: just use a semiconductor device simulator with a very fine grid. — Not possible.

We use the Poisson equation in the form:

$$-\nabla \cdot (\epsilon(\mathbf{x}) \nabla) V(\mathbf{x}) = n(\mathbf{x})$$

$$n(r, \phi, z) := \begin{cases} \text{fast-varying} \\ \chi(r, \phi, z) & \text{for } r > r_1, \\ n_{<}(r, \phi, z) & \text{for } r < r_1 \\ \text{doping} \end{cases}$$



Theorem for the limiting problem $\lambda \rightarrow 0$

Theorem 1 (Heitzinger, Mauser, Ringhofer, 2007). Let $R := [0, r_2]$, $L := [0, 2\pi) \times [0, L_z]$, and $\Omega := R \times L \subset \mathbb{R}^3$. Let $r_1 \in (0, r_2)$, let $\epsilon : R \rightarrow \mathbb{R}^+$ with

$$\epsilon(r) = \begin{cases} \epsilon_{<} \in \mathbb{R} & \text{for } r < r_1, \\ \epsilon_{>} \in \mathbb{R} & \text{for } r > r_1, \end{cases}$$

and let $n \in L^2(\Omega)$ with

$$n(r, \mathbf{y}) := \begin{cases} n_{<}(r, \mathbf{y}) \in L^2([0, r_1) \times L) & \text{for } r < r_1, \\ \chi(r, \mathbf{y}) \in L^2((r_1, r_2) \times L) & \text{for } r > r_1, \end{cases}$$

where $n_{<}$ is bounded and χ is a boundary layer function such that $C(\mathbf{y})$ and $D_r(\mathbf{y})$ exist.

The limiting problem for $\lambda \rightarrow 0$ of the boundary value problem

$$-\nabla \cdot (\epsilon(r) \nabla) V(r, \mathbf{y}) = n(r, \mathbf{y}), \quad (1a)$$

$$V(r_1-, \mathbf{y}) = V(r_1+, \mathbf{y}), \quad (1b)$$

$$\epsilon_{<} \partial_r V(r_1-, \mathbf{y}) = \epsilon_{>} \partial_r V(r_1+, \mathbf{y}) \quad (1c)$$

with $(r, \mathbf{y}) \in \Omega$ is the boundary value problem

$$-\epsilon_{<} \left(\frac{1}{r} \partial_r (r \partial_r) + \frac{1}{r^2} \partial_{\phi\phi} + \partial_{zz} \right) V_h(r, \mathbf{y}) = n_{<}(r, \mathbf{y}) \quad \text{for } r < r_1, \quad (2a)$$

$$-\epsilon_{>} \left(\frac{1}{r} \partial_r (r \partial_r) + \frac{1}{r^2} \partial_{\phi\phi} + \partial_{zz} \right) V_h(r, \mathbf{y}) = 0 \quad \text{for } r > r_1 \quad (2b)$$

with the interface conditions

$$V_h(r_1+, \mathbf{y}) - V_h(r_1-, \mathbf{y}) = \frac{D_r(\mathbf{y})}{\epsilon_{>}}, \quad (3a)$$

$$\epsilon_{>} \partial_r V_h(r_1+, \mathbf{y}) - \epsilon_{<} \partial_r V_h(r_1-, \mathbf{y}) = -C(\mathbf{y}). \quad (3b)$$

λ ($\lambda \rightarrow 0$) is the spatial ratio of one cell to the whole domain.

← The original problem becomes

← the homogenized problem

← with certain interface conditions.



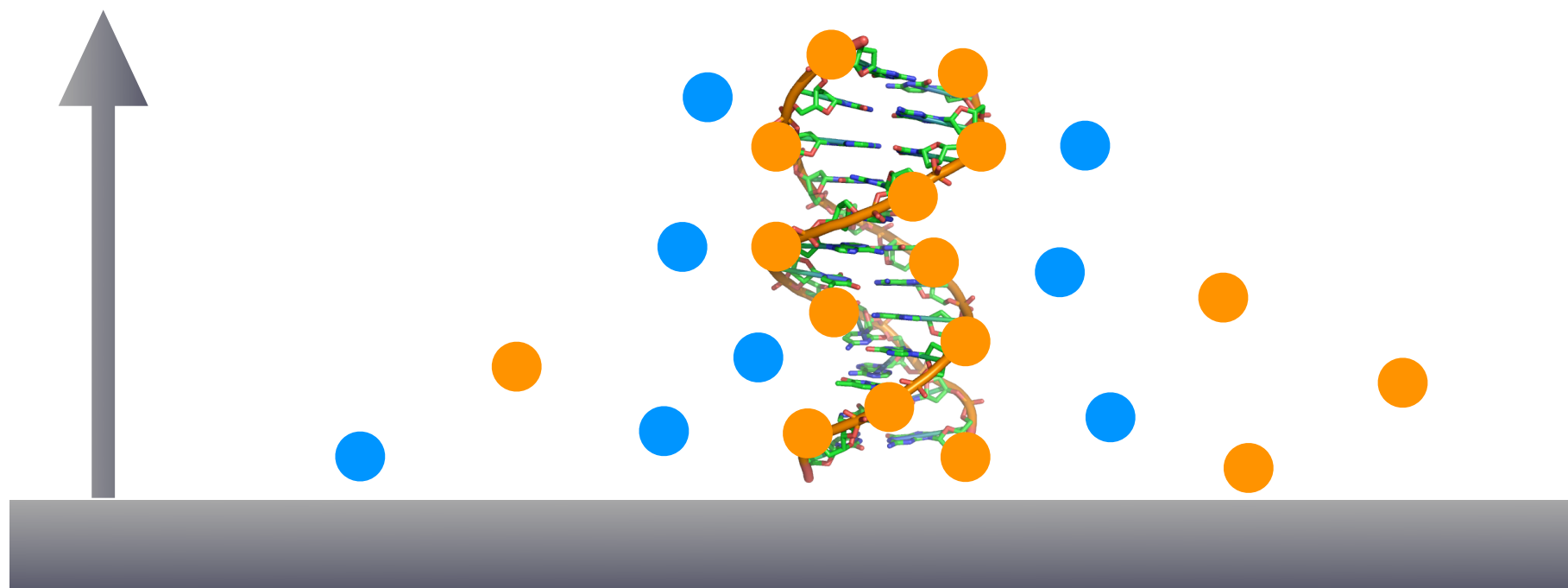
Theorem for the limiting problem $\lambda \rightarrow 0$: what determines the interface conditions?

Definition 1 (Macroscopic surface charge density). *Let χ be a boundary layer function. Then the macroscopic surface charge density $C(\mathbf{y})$ is defined as*

$$C(\mathbf{y}) := \lim_{\lambda \rightarrow 0} \frac{\lambda}{2\pi r_1 L_z} \int_L \int_{r_1}^{r_2} \chi(\rho, \boldsymbol{\eta}, \mathbf{y}) (r_1 + \lambda(\rho - r_1)) d\rho d\boldsymbol{\eta}. \quad (1)$$

Definition 2 (Macroscopic dipole moment density). *Let χ be a boundary layer function. The macroscopic dipole moment density $D(\mathbf{y})$ is defined as*

$$D(\mathbf{y}) := \begin{pmatrix} D_r(\mathbf{y}) \\ D_{\mathbf{y}}(\mathbf{y}) \end{pmatrix} := \lim_{\lambda \rightarrow 0} \frac{\lambda^2}{2\pi r_1 L_z} \int_L \int_{r_1}^{r_2} \begin{pmatrix} \rho - r_1 \\ \boldsymbol{\eta} \end{pmatrix} \chi(\rho, \boldsymbol{\eta}, \mathbf{y}) (r_1 + \lambda(\rho - r_1)) d\rho d\boldsymbol{\eta}. \quad (2)$$



Outline of the proof

Let λ be the spatial ratio of one cell to the whole domain.

If the solution of the PBE converges weakly to a solution V_h for $\lambda \rightarrow 0$, then V_h satisfies a homogenized problem with interface conditions.

Homogenization procedure:

- The functionalized surface is split into cells.
- In each box of length λ , the charge densities and dipole moments of the molecules and the ions in the solution are calculated.
- The jump in the permittivity at the interface is removed by stretching the r -coordinate.
- The problem is converted to its weak formulation.
- The limit $\lambda \rightarrow 0$ is calculated using Taylor expansions.
- Finally the weak formulation is converted back to a strong formulation.



How can we calculate the charge densities and dipole moments of the boundary layer?

We construct B-DNA strands from the coordinates of single nucleotides.

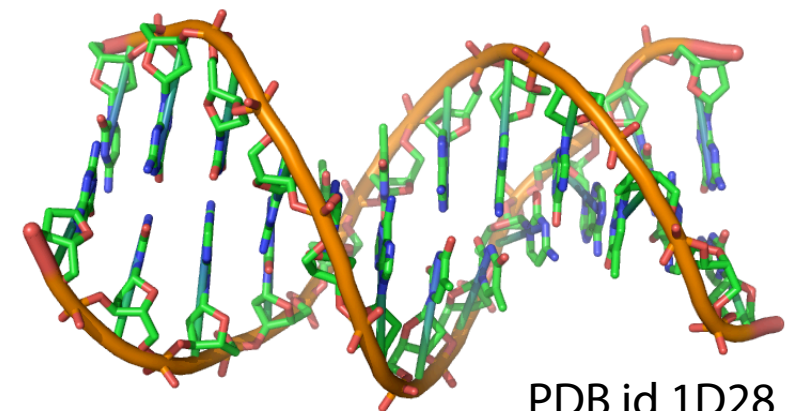
Arbitrary sequences, linker lengths, and orientations with respect to the surface are possible.

We use a GROMACS force field to obtain the partial charges of the probe and target molecules (and the locations of the hydrogens).

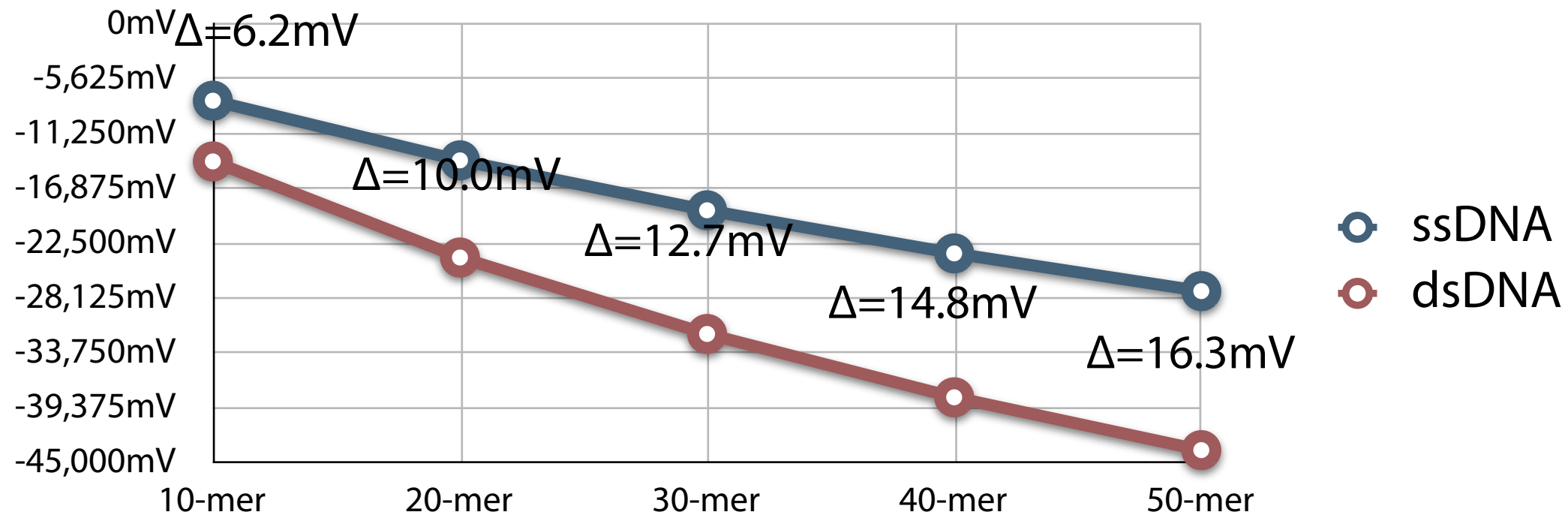
The same procedure can be used for any biomolecule whose structure is known (see PDB, for example).

To calculate the electrostatics and charge distributions, we are using two methods:

- solve the Poisson-Boltzmann equation or
- perform Metropolis Monte Carlo calculations.



1D simulation of nanoplates and different DNA strand lengths



1D simulation of a nanoplate DNA-FET:

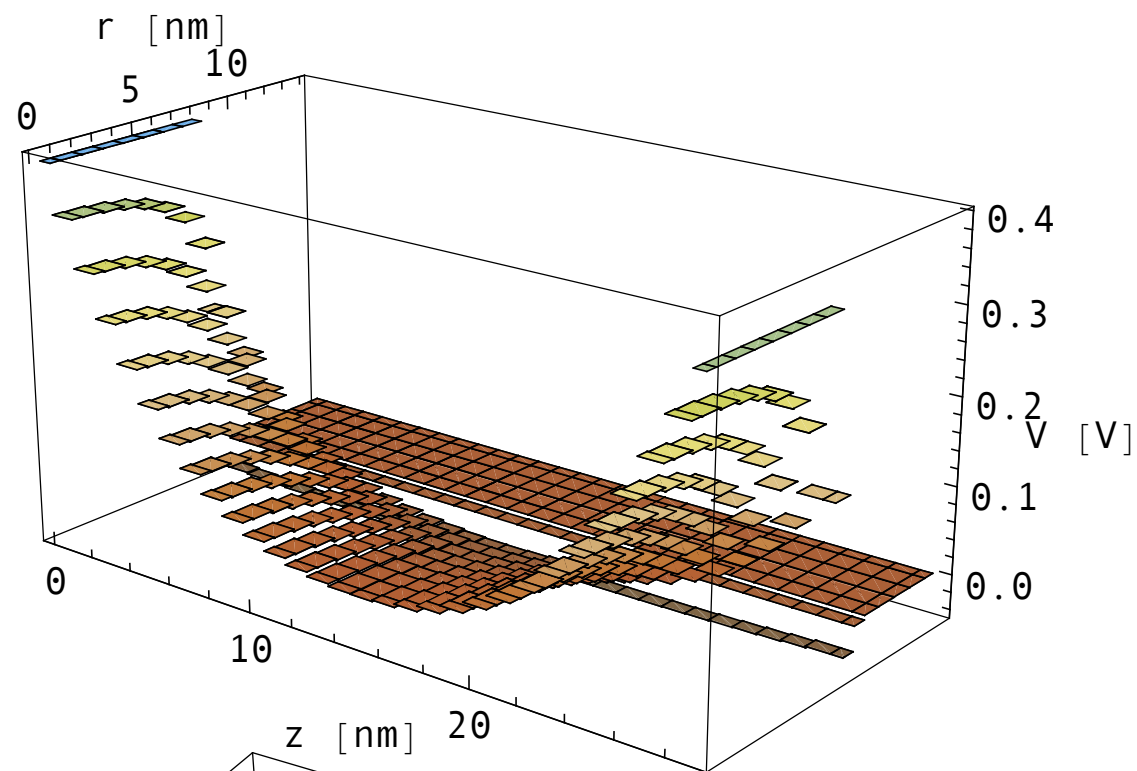
- Binding efficiency: 100%;
oxide thickness: 2nm; Si nanoplate thickness: 30nm.

Experimental data from Fritz et al., PNAS 99 2002:

- Oxide thickness: 2nm;
12-mer oligonucleotides;
surface potential change: about 5mV depending on concentration (i.e., binding efficiency).



Self-consistent simulations using the drift-diffusion model for a silicon-nanowire sensor

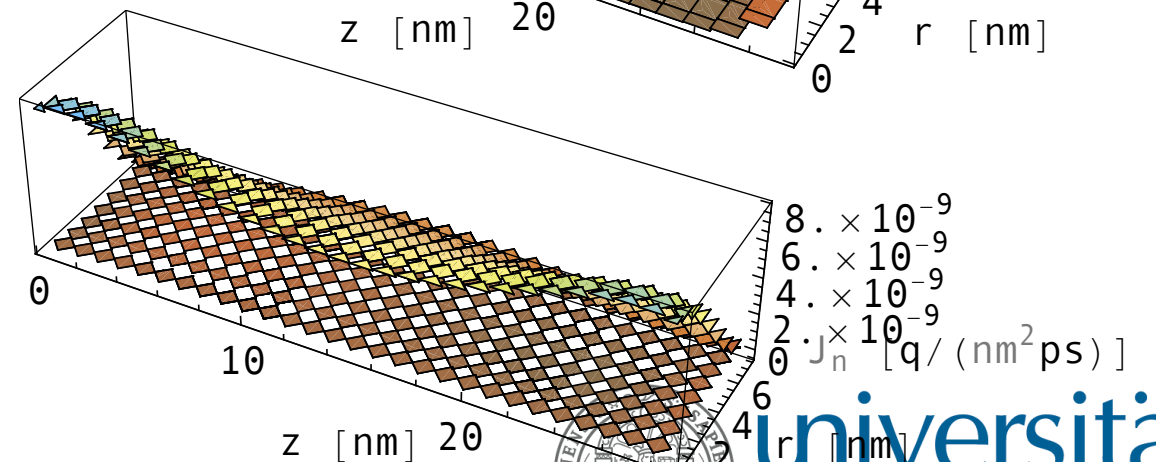
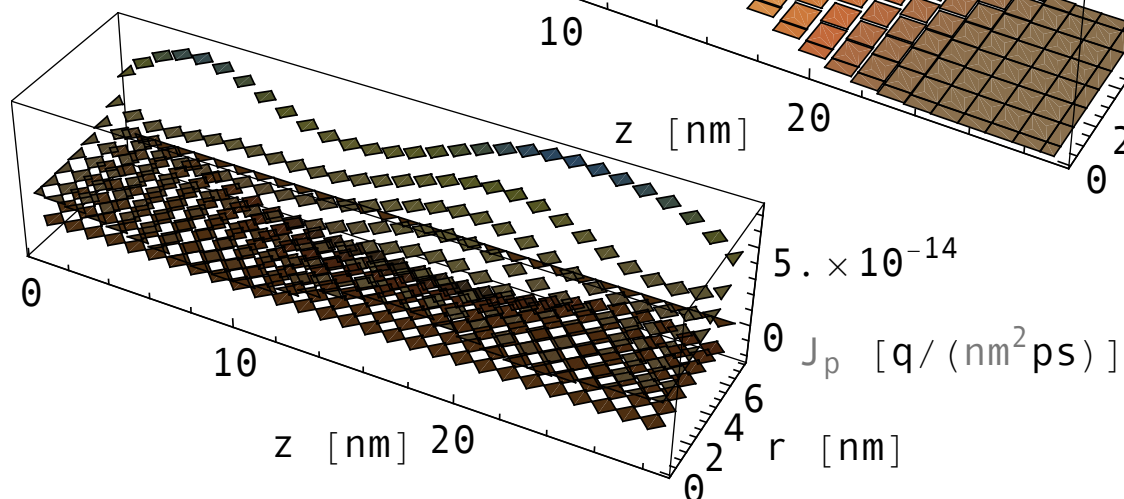
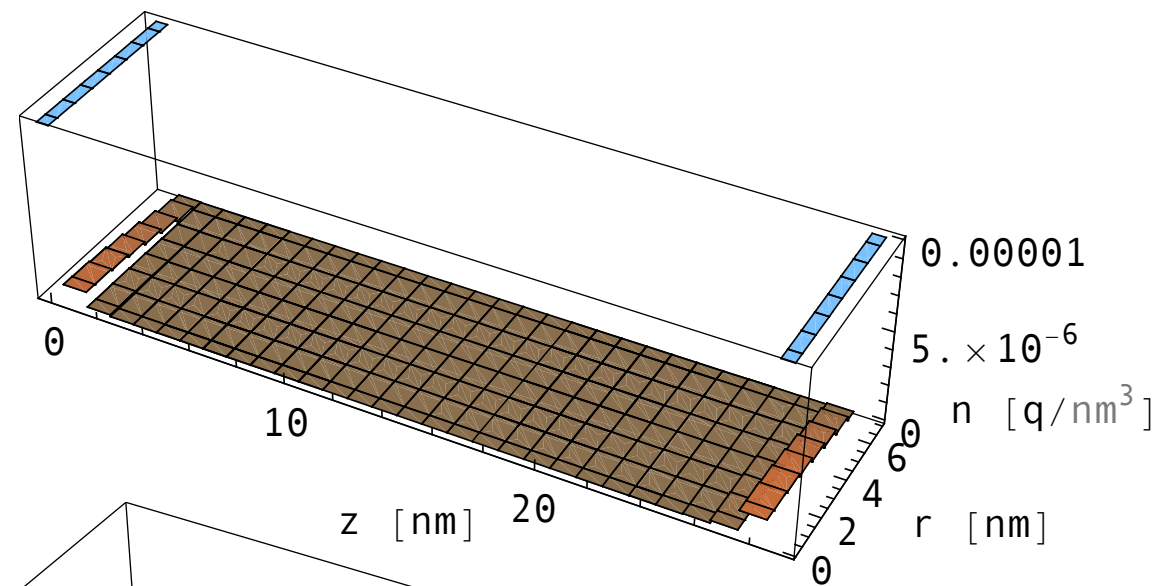
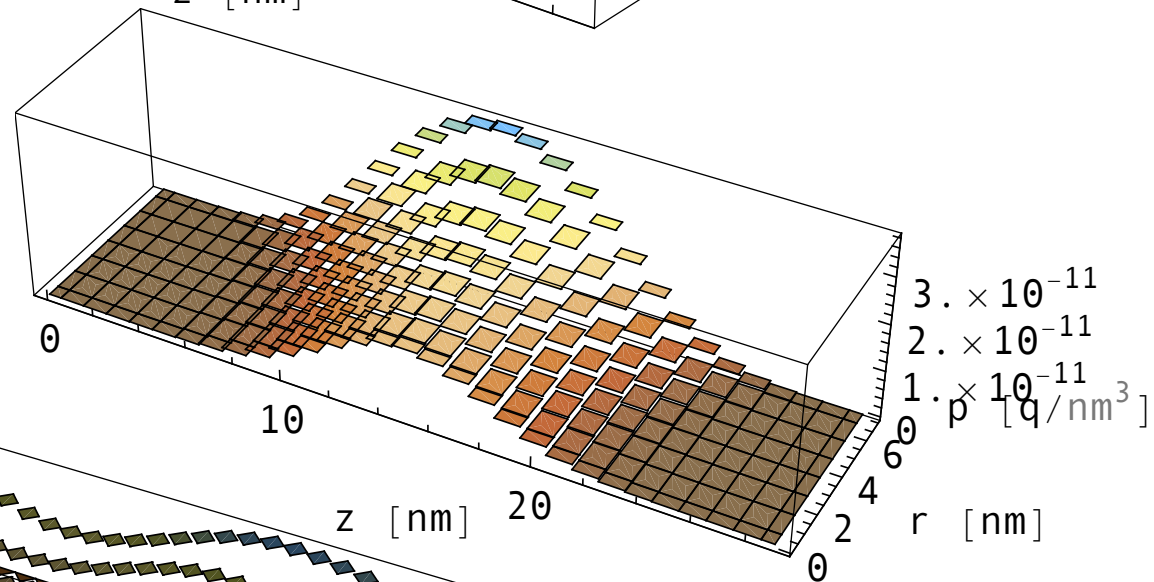


$$J_n = -q\mu_n n \nabla V + qD_n \nabla n$$

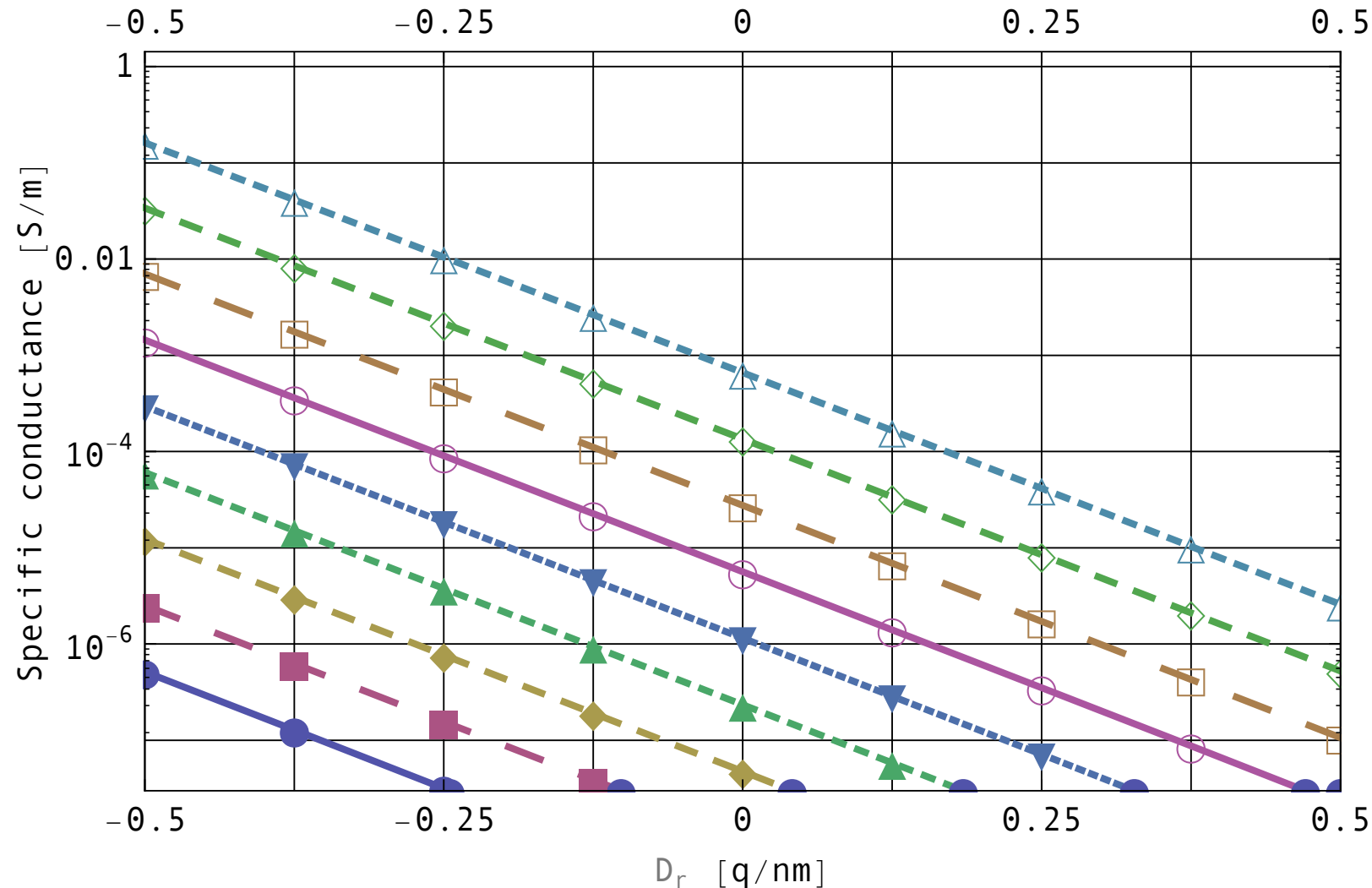
$$J_p = -q\mu_p p \nabla V - qD_p \nabla p$$

$$\nabla \cdot J_n = q\partial_t n + qR$$

$$\nabla \cdot J_p = -q\partial_t p - qR$$



Conductance of a silicon-nanowire sensor



The bottom line (blue, solid line with solid circles) is for $C = -0.5 \text{ q/nm}^2$.

The top line (light blue, dashed line with hollow triangles) is for $C = +0.5 \text{ q/nm}^2$.

Step size in C : 0.125 q/nm^2 .

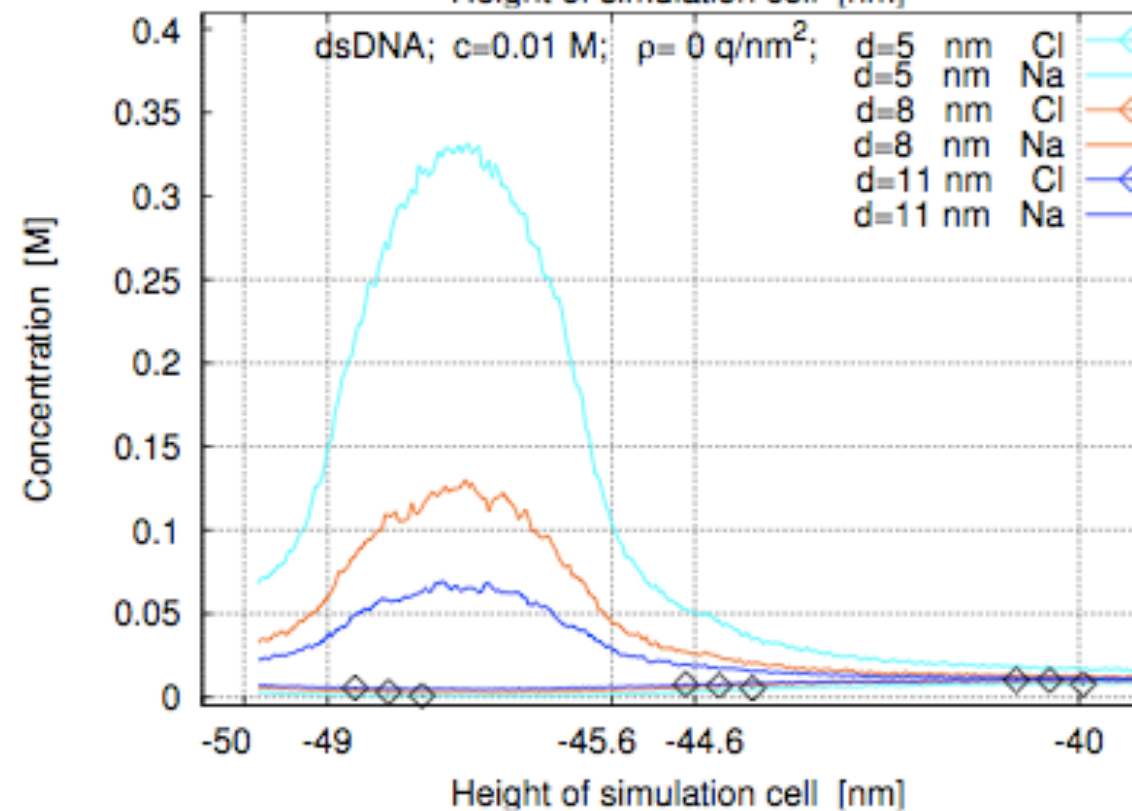
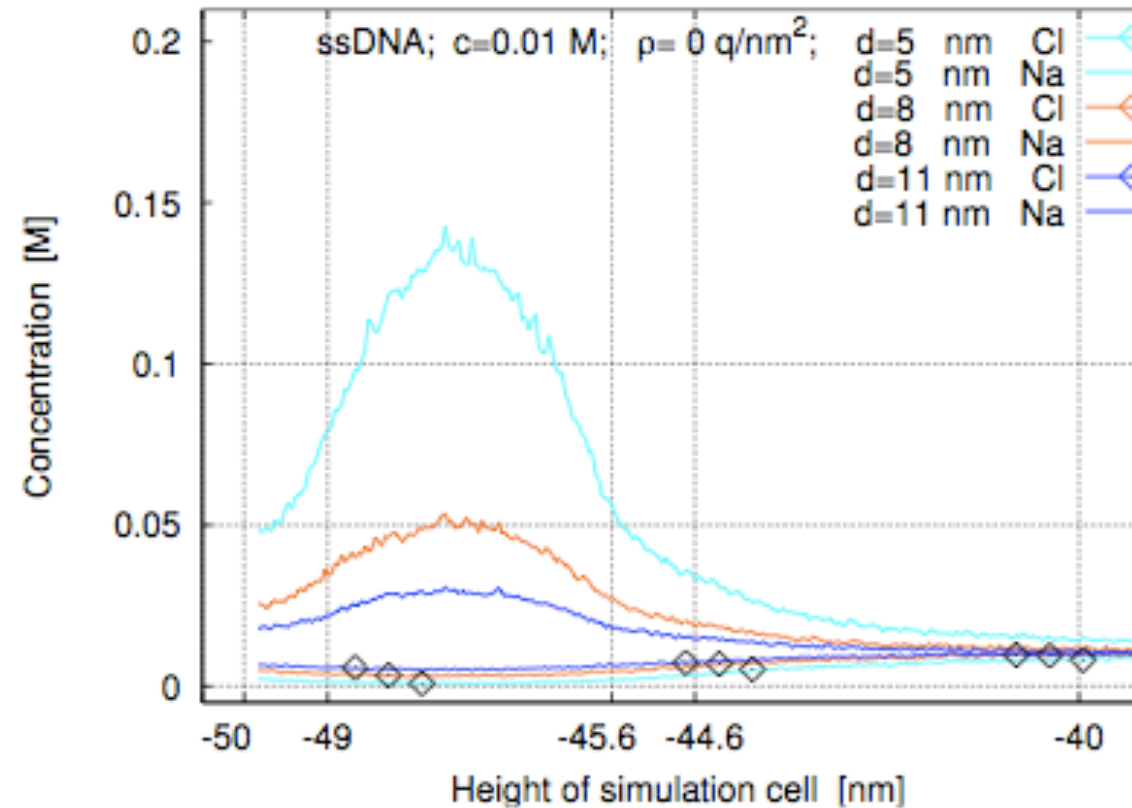
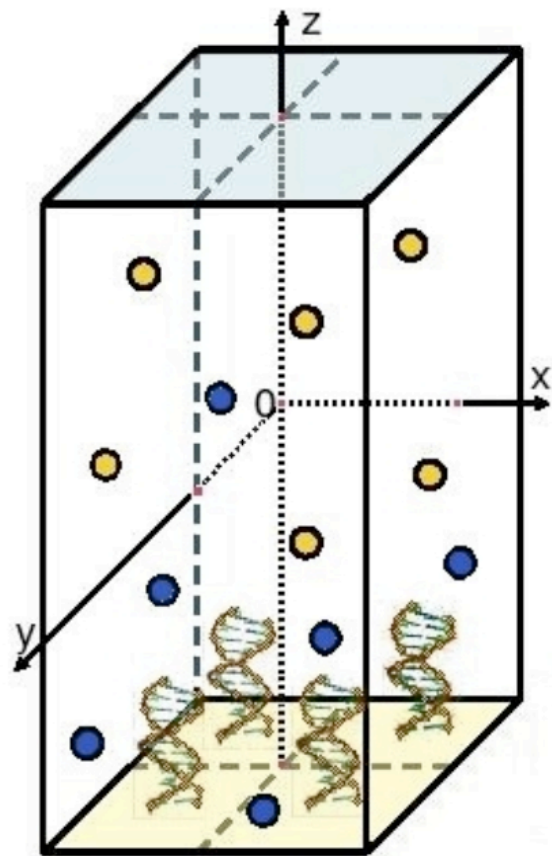
We homogenized the Poisson equation for cylindrical geometries as well.

Here the specific conductance (from the 2D DD model) is shown as a function of the dipole moment density of the biofunctionalized layer.

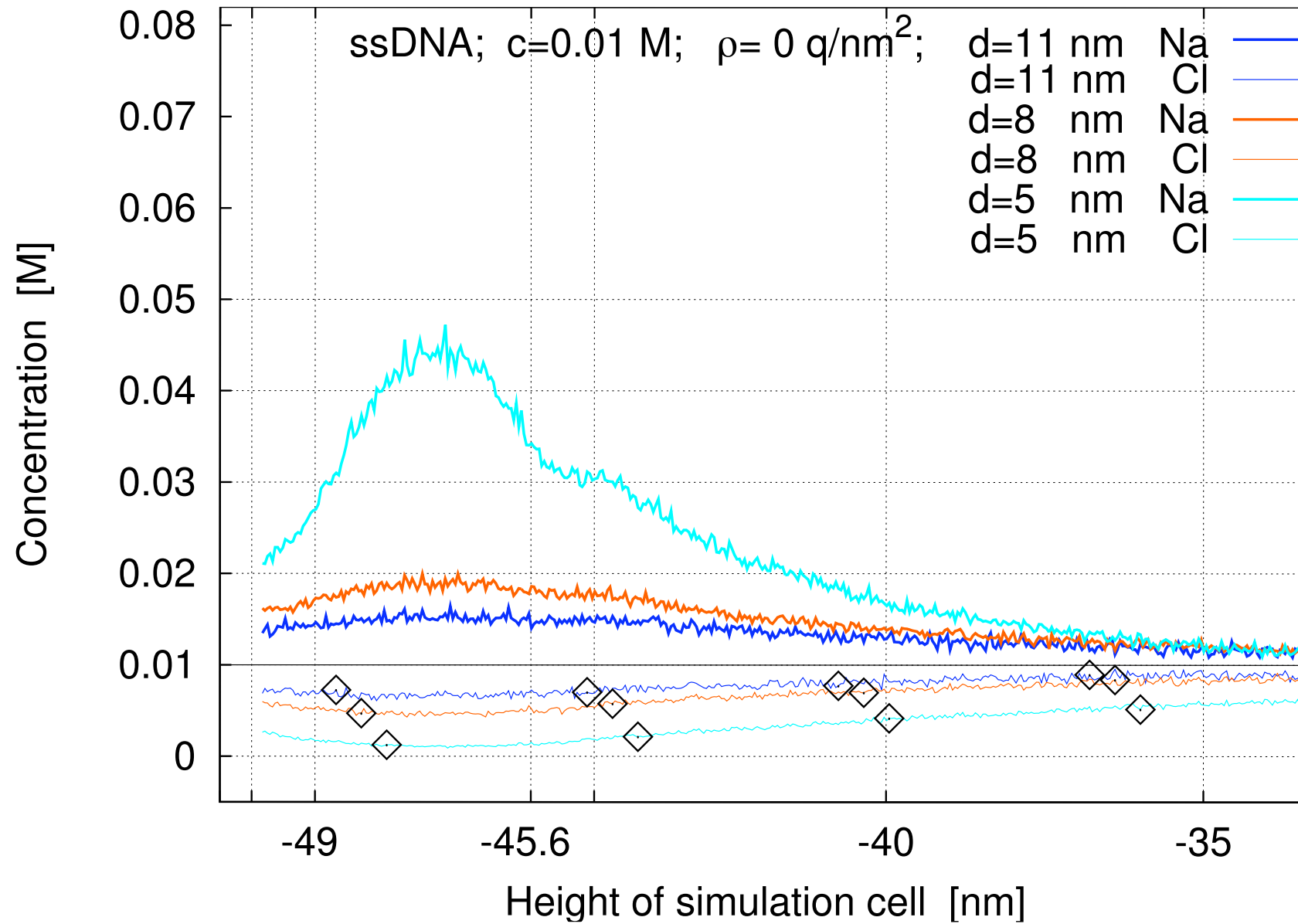
The liquid contains 10^{-6} mol/L of Na^+Cl^- . The p-doped (10^{16} cm^{-3}) Si nanowire is 100nm long, the silicon core has a radius of 5nm, and the silicon oxide layer has a thickness of 2nm.



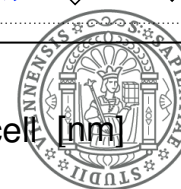
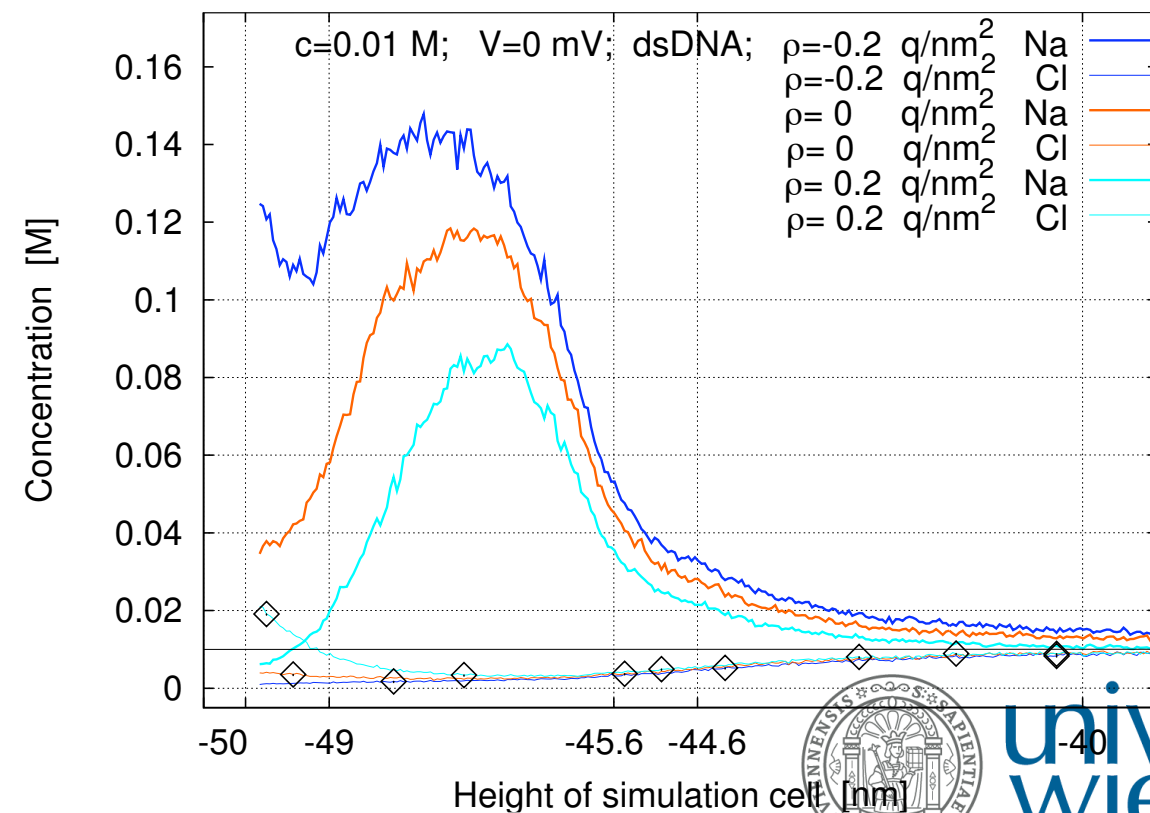
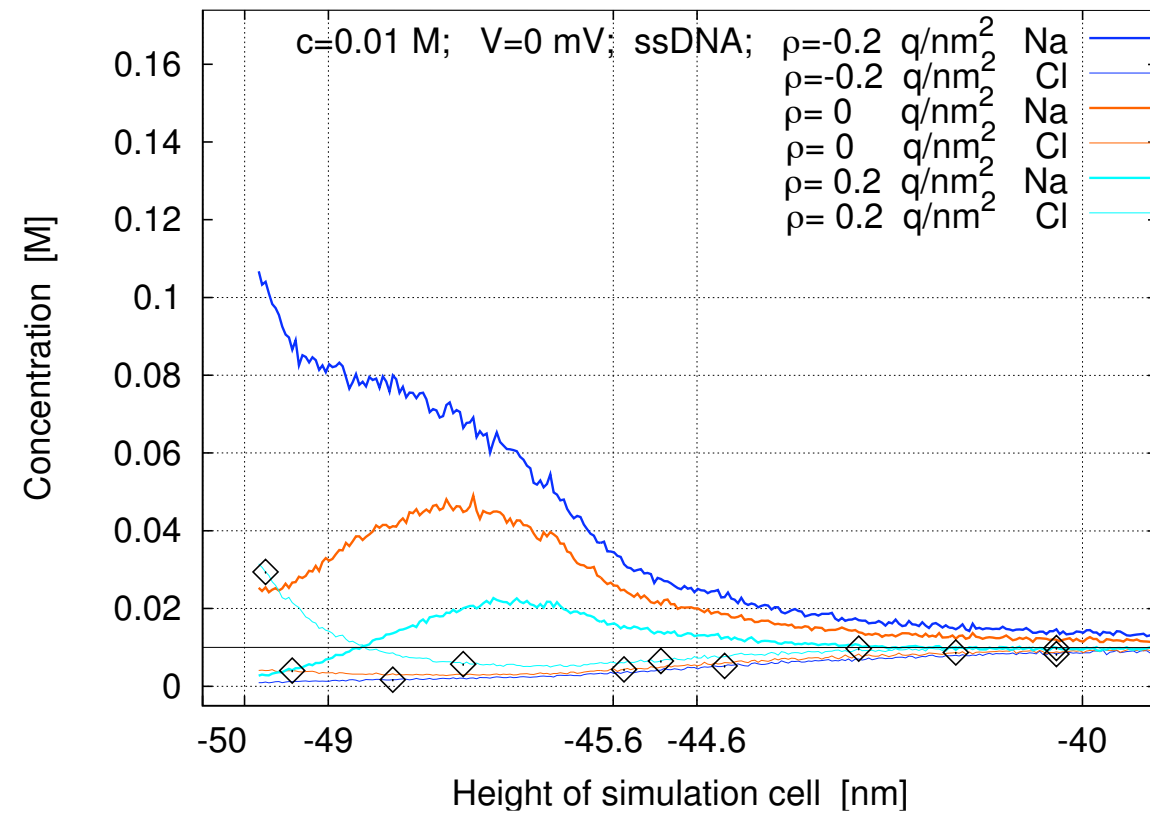
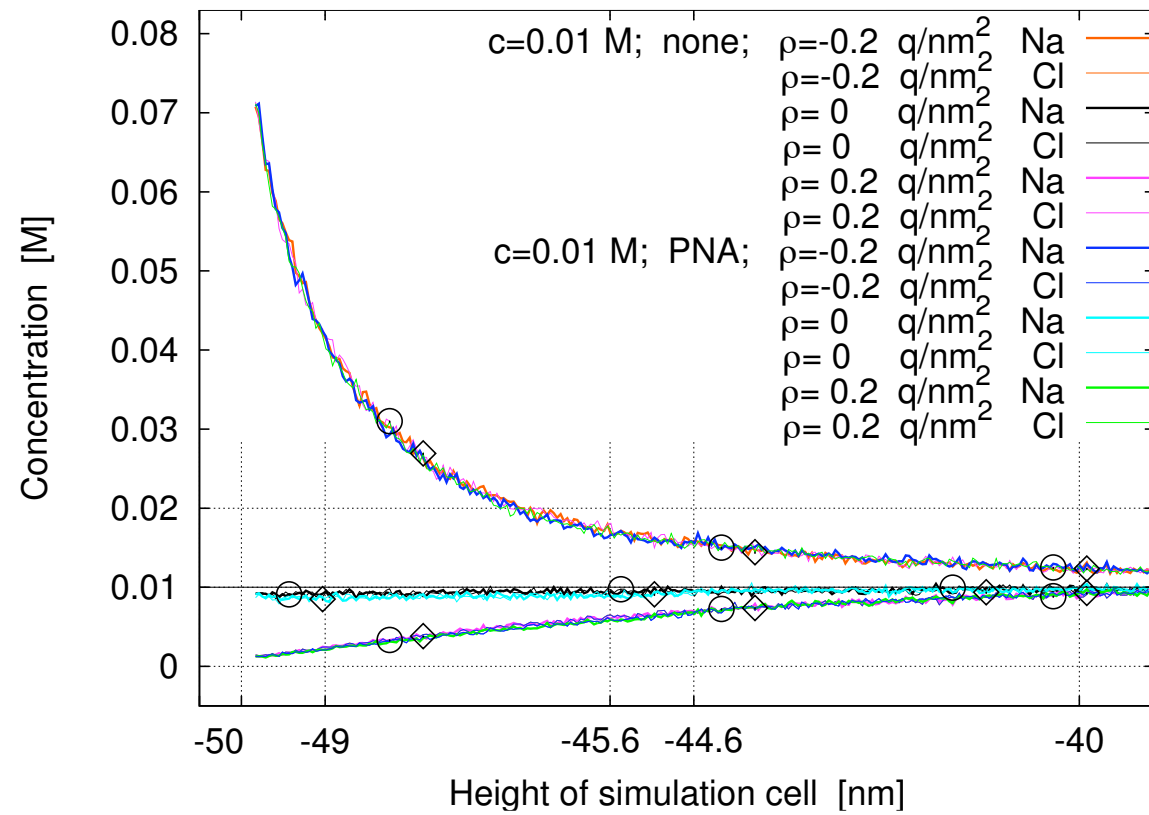
MC simulations of the surface layer: the electric double layer, PNA, ssDNA, & dsDNA



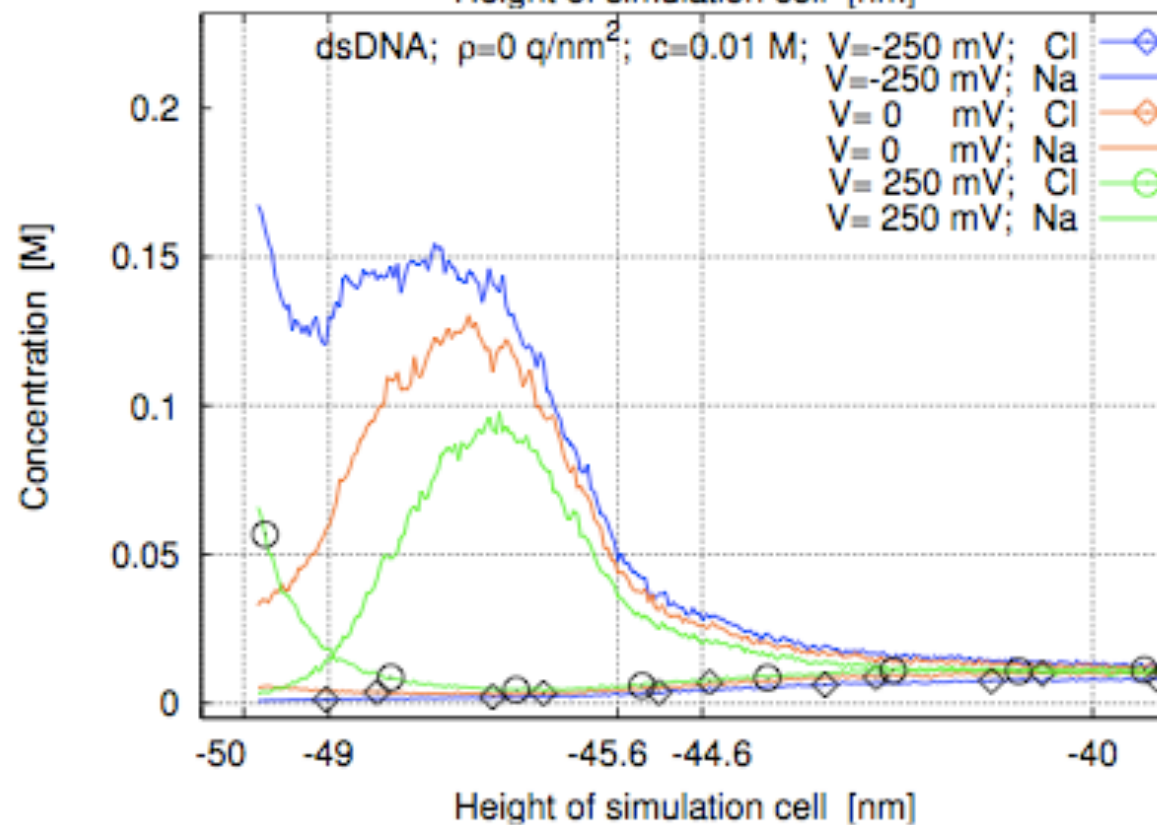
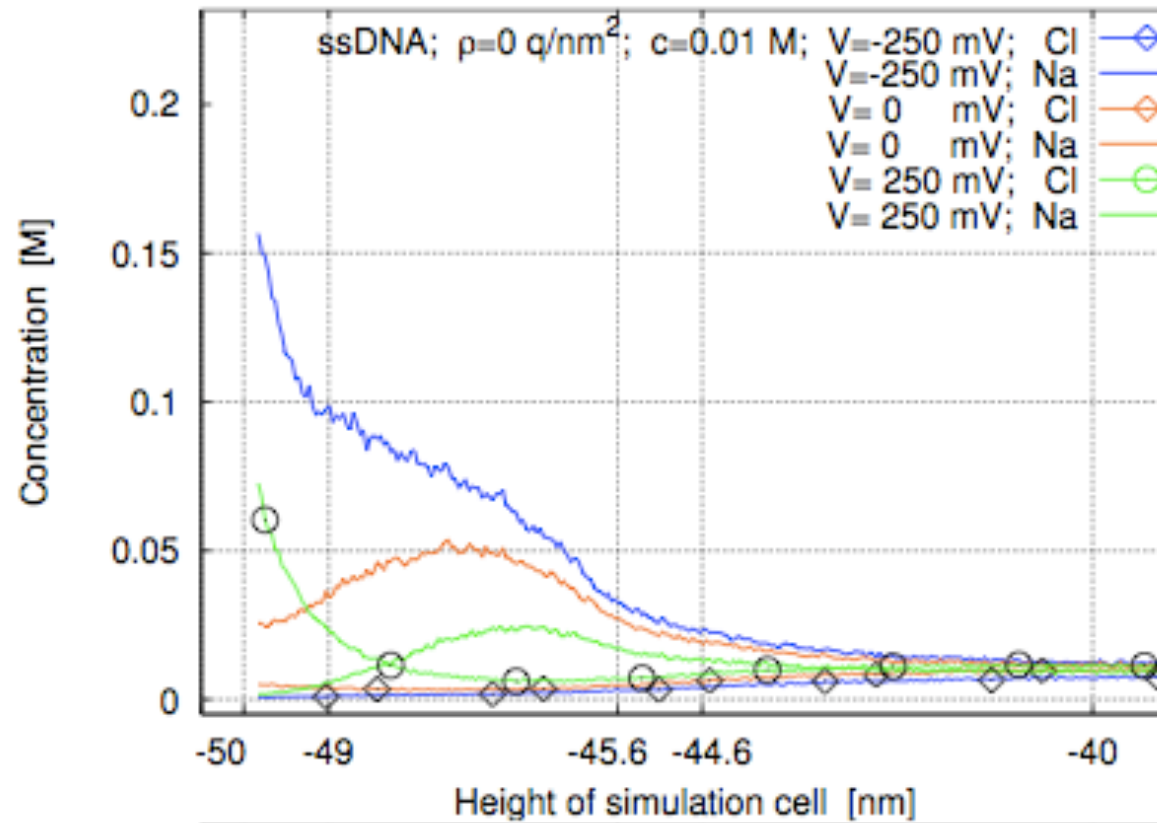
MC simulations: the influence of probe spacing



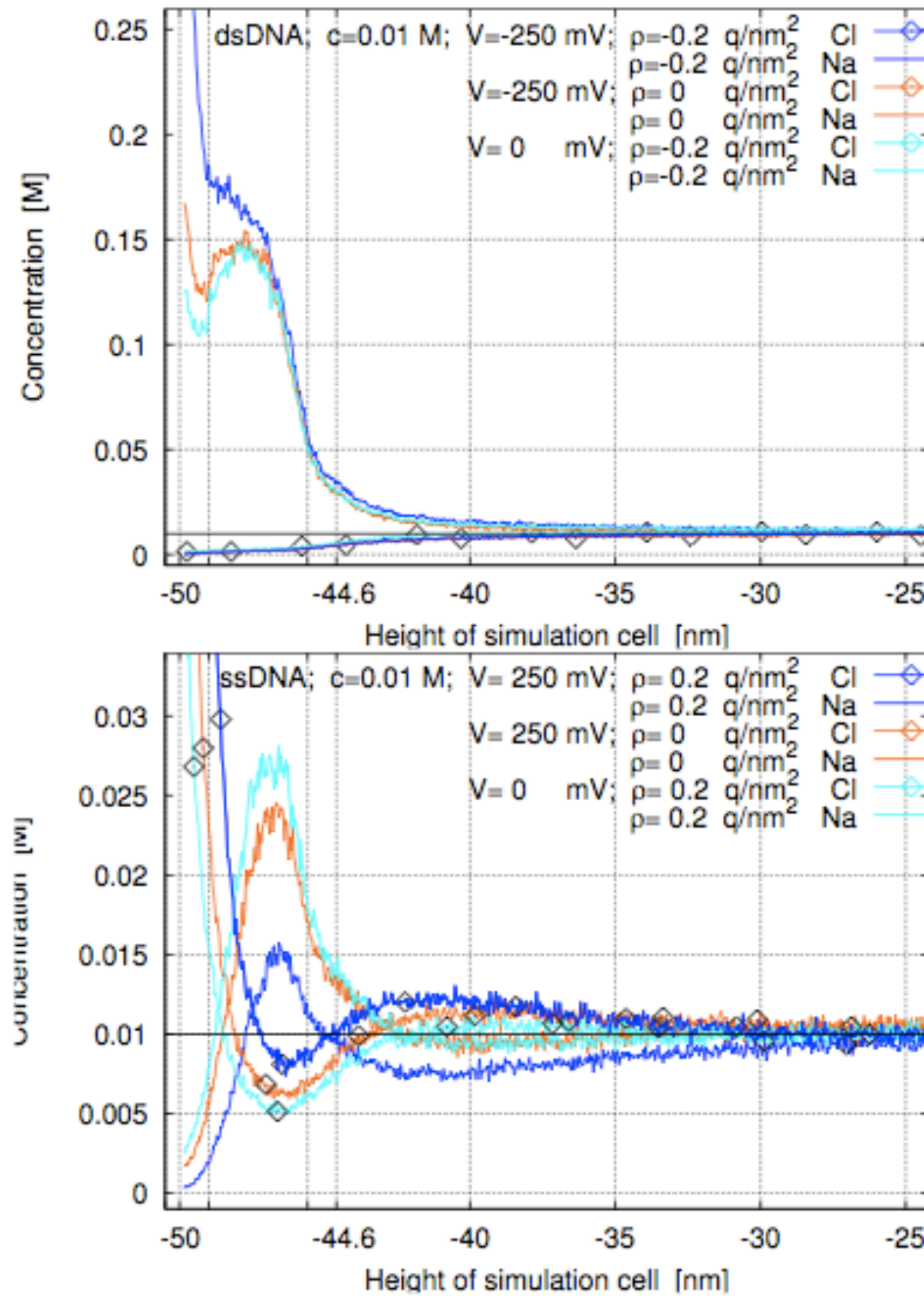
MC simulations: the influence of surface (oxide) charge density



MC simulations: the influence of applied voltage



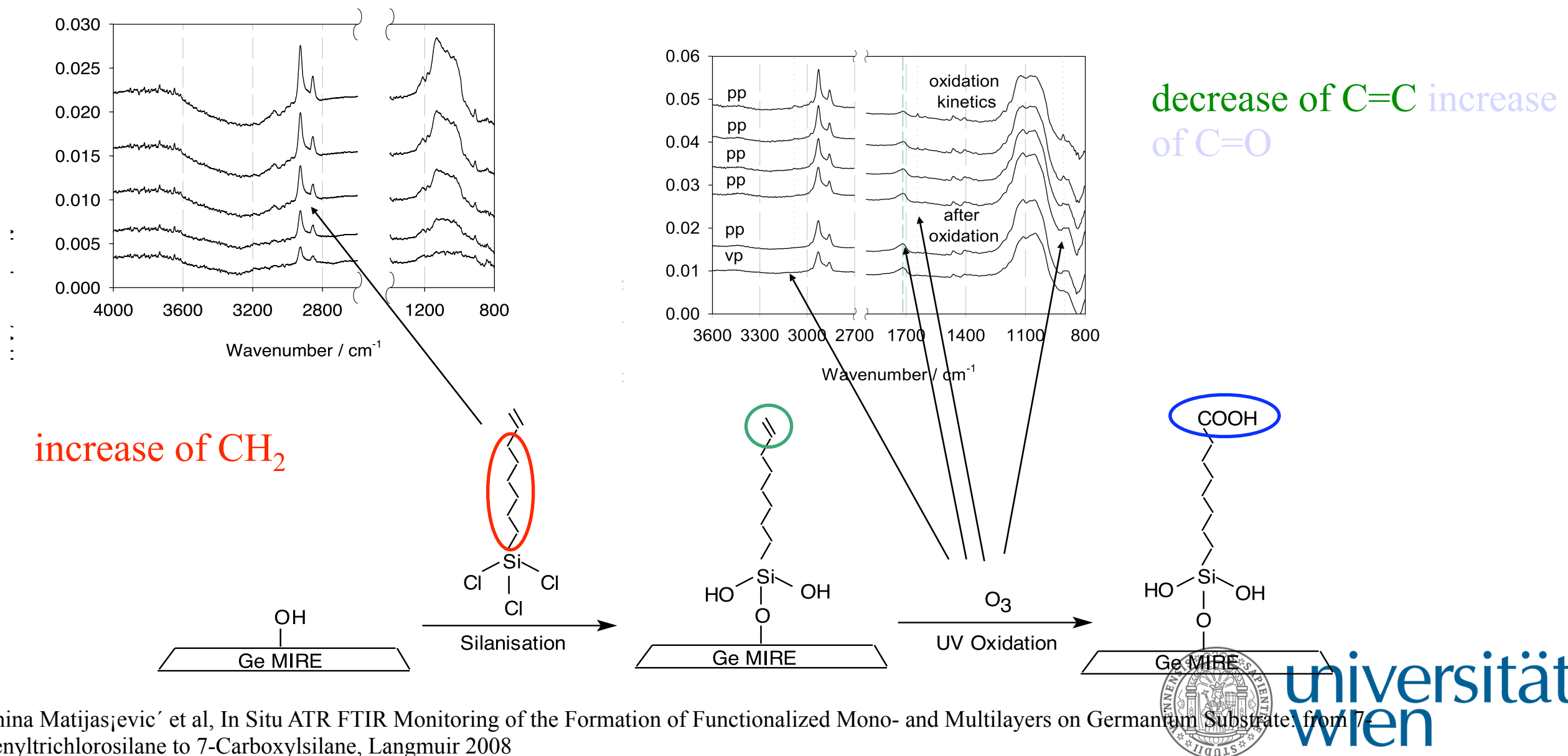
MC simulations: three-layer behavior



FTIR ATR spectroscopy can measure molecule density and orientation

Fourier-transformed infrared attenuated total reflection spectroscopy provides in-situ quantitative information about molecules (chemical bonds) at a Si or Ge wafer and (possibly) about their orientations.

Collaboration with Dieter Baurecht's group (U. of Vienna).

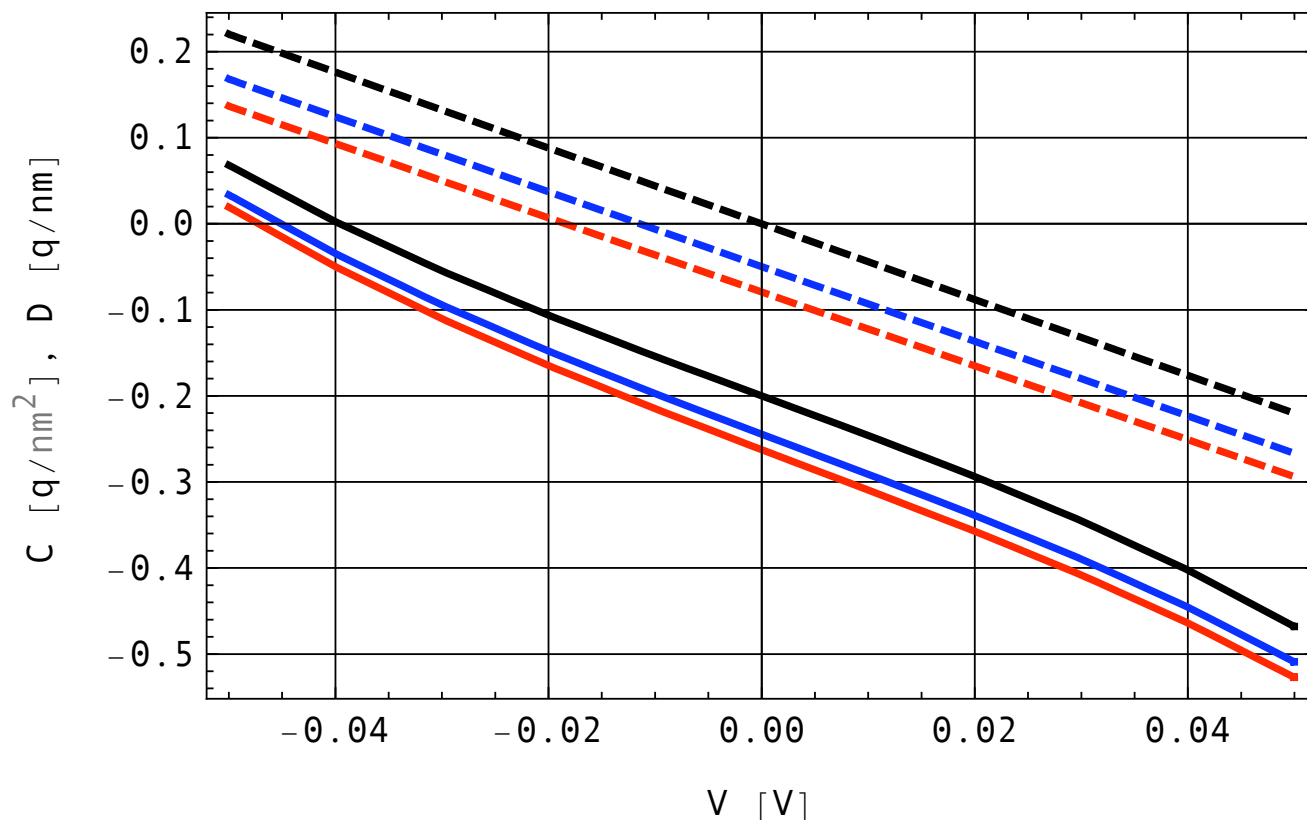


Self-consistent loop between microscopic (PB) and macroscopic (DD) simulations

The microscopic model is the Poisson–Boltzmann equation:
 surface charge density $-0.2q/\text{nm}^2$, 5nm boxes, 100mM NaCl,
 C...solid lines, D...dashed lines,
 no molecule...black lines, ssDNA...blue lines, dsDNA...red lines.

The macroscopic model is drift-diffusion for a silicon nanowire.

No fitting parameters!



Boundary layer	Specific conductance	
No molecules	2.29E-6 S/m	0%
ssDNA	2.58E-6 S/m	+12.7%
dsDNA	2.91E-6 S/m	+12.8%

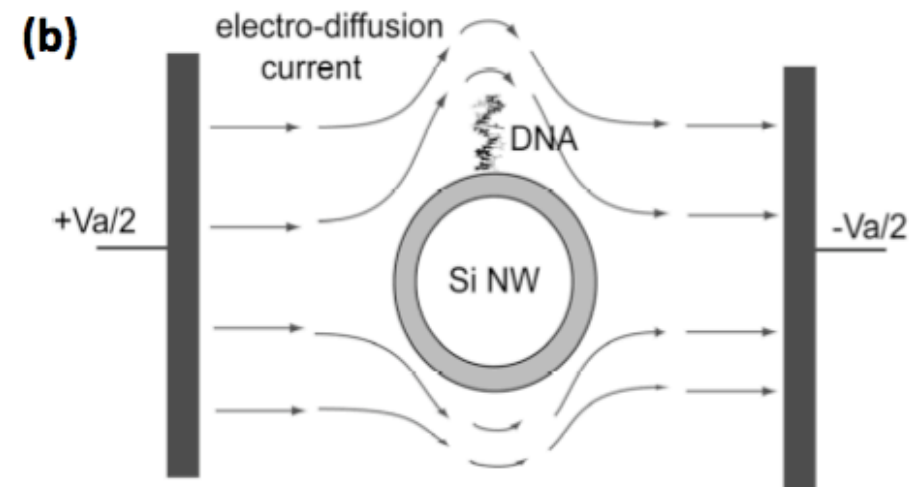
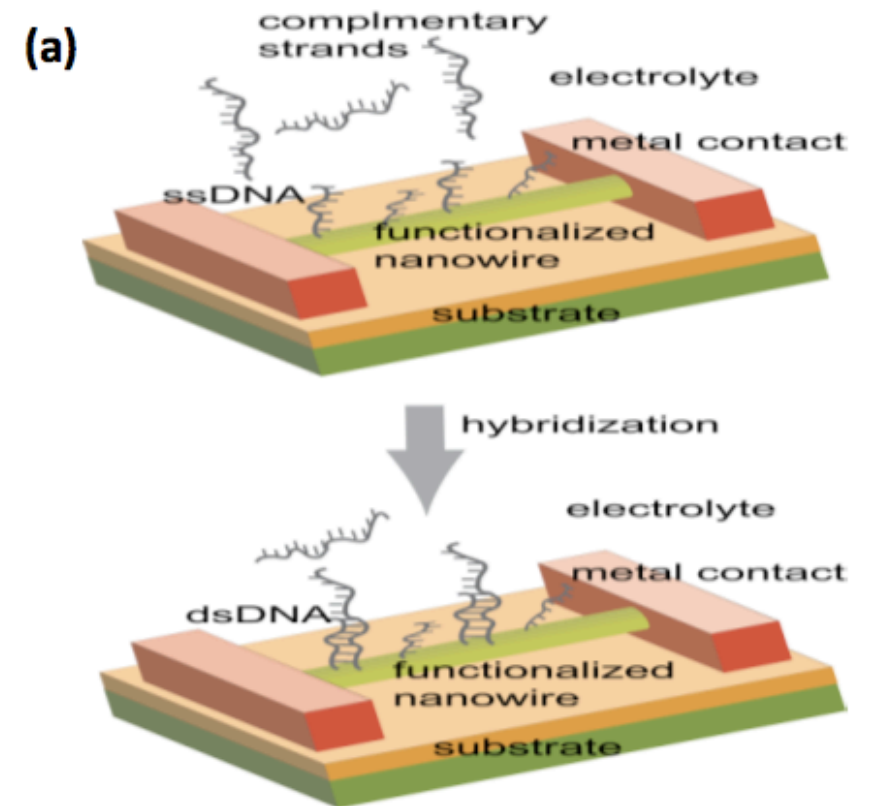


How to overcome the screening-induced performance limits of field-effect biosensors

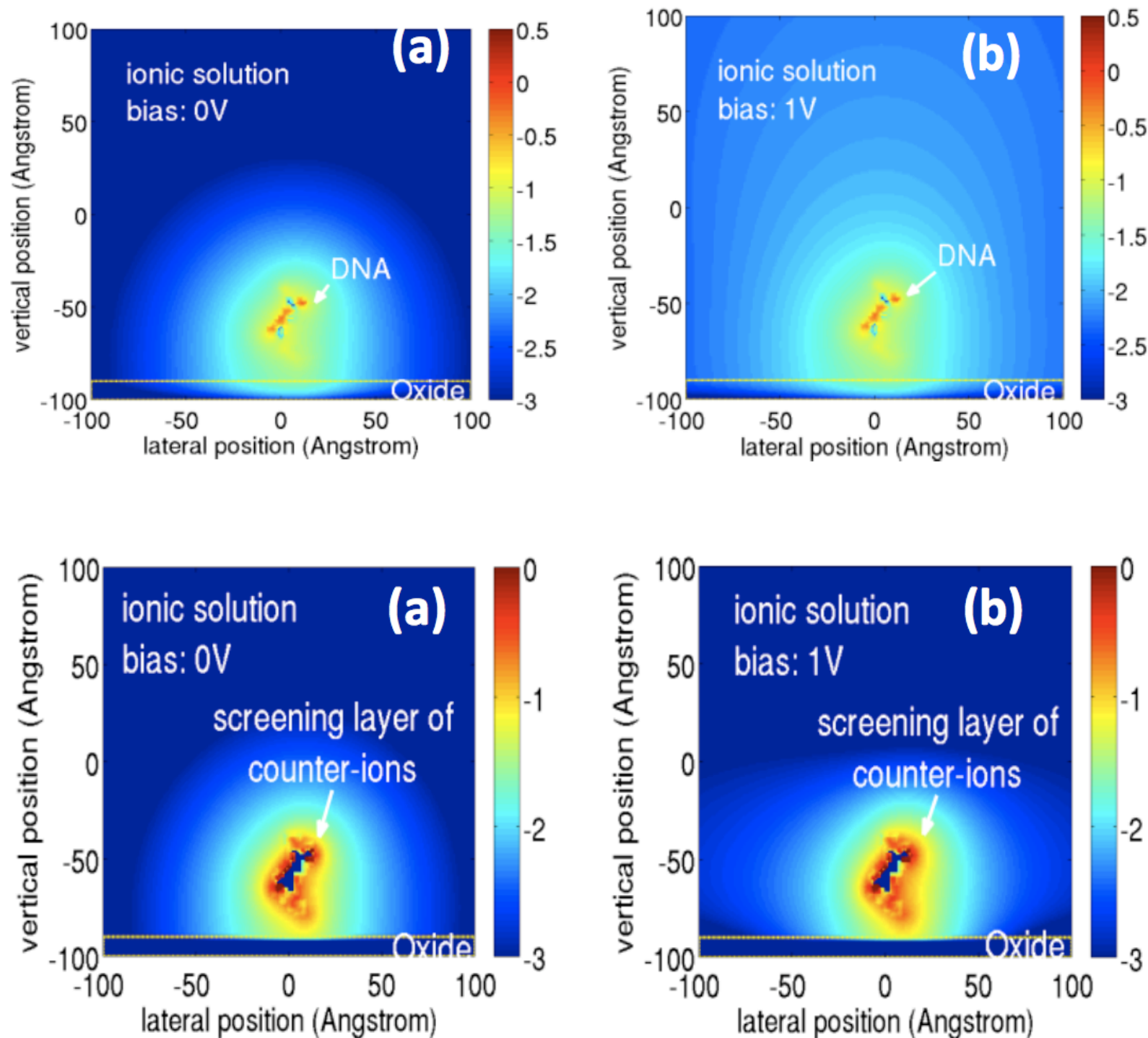
The performance of field-effect sensors is limited by the screening of the partial charges of the biomolecules by the (counter-)ions in the liquid.

How can we increase the Debye length?

New idea:
what happens if we add an **electro-diffusion current**?



How to overcome the screening-induced performance limits of field-effect biosensors (2d)

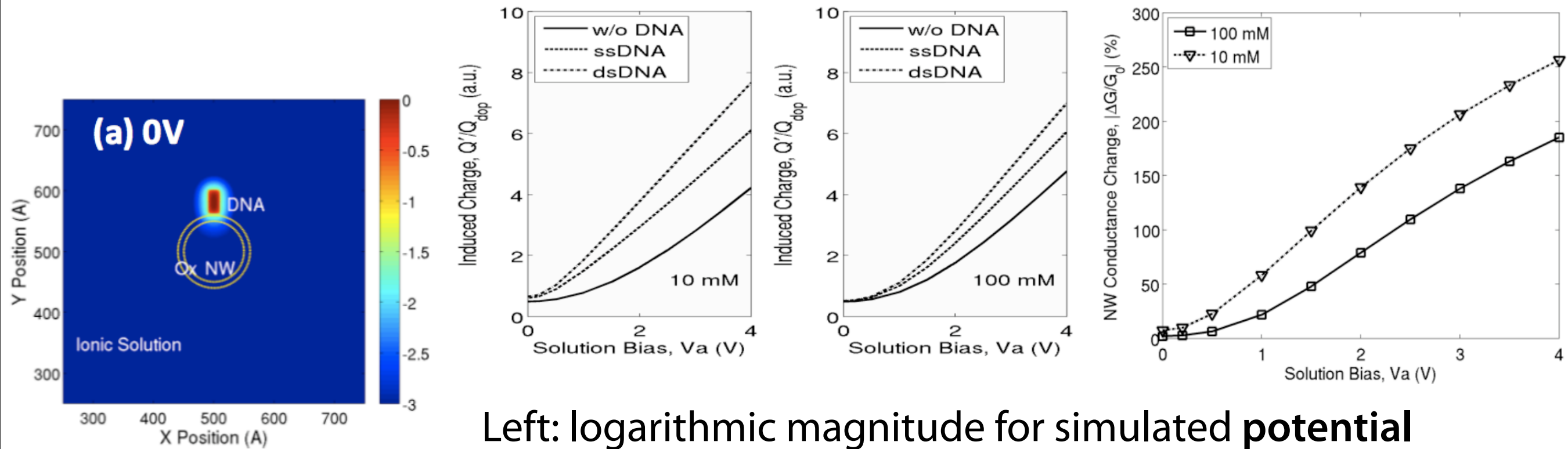


Logarithmic magnitude of the **simulated potential change** (top) and of the **simulated cation density change** (bottom) at a vertical cut-plane of the structure for (a) 0V and (b) 1V electrolyte bias.

The potential change is obtained as the potential difference between the cases with or without a 12 base-pair DNA at the center.



How to overcome the screening-induced performance limits of field-effect biosensors (3d)



Left: logarithmic magnitude for simulated **potential change** at a lateral cut-plane for (a) 0V and (b) 1V.

Top left: **charge induced** in silicon nanowire (normalized by doping) as a function of electrolyte biases (10mM and 100mM).

Top right: (normalized) silicon nanowire **conductance** change between ssDNA and dsDNA cases as a function of electrolyte biases. At 1V, **enhancement factors of 11x** (at 100mM) and **8x** (at 10mM) are seen.



Conclusion

The problem:

- **Field-effect** nano-biosensors are a technology with many biomedical applications. How they work has not been understood at a **quantitative** level.
- Due to the different length scales of biomolecules and sensor areas (4 or 5 orders of magnitude), **multi-scale modeling** is necessary.

The solution:

- We have solved the multi-scale problem by deriving **homogenized interface conditions** for nanoplate and nanowire geometries.
- Our models enable the **self-consistent** simulation of all the charges in the devices. This makes **predictive** investigations possible.
- There are **no fitting parameters** in the model.
- Good **agreement with experiments** has been found.
- A numerical study has shown how **screening-induced performance limits** can be overcome.

We can now **calculate** what could not be calculated previously.





Prof. Norbert **Mauser**
*Department of Mathematics & Wolfgang Pauli Institute,
University of Vienna*



Prof. Christoph **Überhuber**
*Institute for Analysis and Scientific Computing,
TU Vienna*



Mag. Alena **Bulyha** (doctorate student)
*Department of Mathematics & Wolfgang Pauli Institute,
University of Vienna*



Stefan **Baumgartner** (master's student)
*Department of Mathematics & Wolfgang Pauli Institute,
University of Vienna*



Prof. Dieter **Baurecht**
*Institute for Biophysical Chemistry,
University of Vienna*



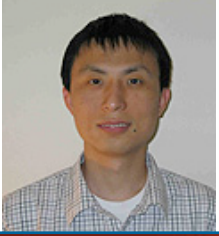
Prof. Heidrun **Karlic**
*Institute for Leukemia Research and Hematology,
Ludwig Boltzmann Society, Vienna*



Dr. Franz **Varga**
*Institute for Osteology,
Ludwig Boltzmann Society, Vienna*

Mag. Manuel **Punzet** (doctorate student)
*Institute for Biophysical Chemistry,
University of Vienna*



	<p>Prof. Christian Ringhofer <i>Department of Mathematics and Statistics, Arizona State University, & Wolfgang Pauli Institute, Vienna</i></p>
	<p>Prof. Robert Dutton <i>EE & Center for Integrated Systems, Stanford University</i></p>
	<p>Dr. Yang Liu <i>Center for Integrated Systems, Stanford University</i></p>
	<p>Prof. Deszö Boda <i>Department of Physical Chemistry, University of Pannonia, Hungary</i></p>

	<p>ÖAW (Austrian Academy of Sciences) jubilee-fund project <i>Multi-Scale Modeling and Simulation of Field-Effect Nano-Biosensors</i></p>
	<p>FWF (Austrian Science Fund) project <i>Mathematical Models and Characterization of BioFETs</i></p>

Publications are available at <http://Clemens.Heitzinger.name/>

